INFORMATION TO USERS

This manuscript has been reproduced from the microfilm master. UMI films the text directly from the original or copy submitted. Thus, some thesis and dissertation copies are in typewriter face, while others may be from any type of computer printer.

The quality of this reproduction is dependent upon the quality of the copy submitted. Broken or indistinct print, colored or poor quality illustrations and photographs, print bleedthrough, substandard margins, and improper alignment can adversely affect reproduction.

In the unlikely event that the author did not send UMI a complete manuscript and there are missing pages, these will be noted. Also, if unauthorized copyright material had to be removed, a note will indicate the deletion.

Oversize materials (e.g., maps, drawings, charts) are reproduced by sectioning the original, beginning at the upper left-hand corner and continuing from left to right in equal sections with small overlaps. Each original is also photographed in one exposure and is included in reduced form at the back of the book.

Photographs included in the original manuscript have been reproduced xerographically in this copy. Higher quality 6" x 9" black and white photographic prints are available for any photographs or illustrations appearing in this copy for an additional charge. Contact UMI directly to order.

UMI

A Bell & Howell Information Company
300 North Zeeb Road, Ann Arbor MI 48106-1346 USA
313/761-4700 800/521-0600

Adaptive IIR filtering using the homotopy continuation method

by

Sangmin Bae

A dissertation submitted to the graduate faculty

in partial fulfillment of the requirements for the degree of

DOCTOR OF PHILOSOPHY

Major: Electrical Engineering (Communications and Signal Processing)

Major Professor: Lalita Udpa

Iowa State University

Ames, Iowa

1997

Copyright © Sangmin Bae, 1997. All rights reserved.

UMI Number: 9725390

UMI Microform 9725390
Copyright 1997, by UMI Company. All rights reserved.

This microform edition is protected against unauthorized
copying under Title 17, United States Code.

UMI
300 North Zeeb Road
Ann Arbor, MI 48103

Graduate College
Iowa State University

This is to certify that the Doctoral dissertation of

Sangmin Bae

has met the dissertation requirements of Iowa State University

Signature was redacted for privacy.

Major Professor

Signature was redacted for privacy.

For the Major Program

Signature was redacted for privacy.

For the Graduate College

TABLE OF CONTENTS

LIST OF TABLES

LIST OF FIGURES

ABBREVIATIONS

AHCM - Adaptive Homotopy Continuation Method

AHCMLMS - Adaptive Homotopy Continuation Method Least Mean Square

AR - Auto-Regressive

ARMA - Auto-Regressive and Moving Average

BDE - Basic Differential Equation

FBH - Flat Bottomed Hole

FIR - Finite-length Impulse Response

HCM - Homotopy Continuation Method

HDE - Homotopy Differential Equation

IIR - Infinite-length Impulse Response

LMS - Least Mean Square

MA - Moving Average

MAHCM - Multi-stage Adaptive Homotopy Continuation Method

MSE - Mean Squared Error

MSOE - Mean Squared Output Error

NDE - Nondestructive Evaluation

PC - Prediction-Correction

RLS - Recursive Least Square

1 INTRODUCTION

Adaptive Filtering

The subject of digital filtering is an important topic in the field of signal processing and has justifiably witnessed considerable growth in the last decade. The need for developing more advanced signal processing techniques has been growing to meet the increasing demand arising from rapid expansion in the communication industry. The advantages of using powerful computers and digitized signals have further accelerated research in digital signal processing.

"Filtering" is generally defined as the processing of stochastic signals to extract relevant information from noisy measurements. A stochastic signal describes the time evolution of a statistical phenomenon. The design of filters can be described as an algorithmic procedure that uses the statistical information contained in data and noise to determine the coefficients of the desired filter, by minimizing an appropriate error metric between the desired signal and the filter output.

Broadly, filters can be categorized into linear and non-linear filters depending on a mathematical operator mapping the filter input to output. Each class of filters has its own advantages and disadvantages. A nonlinear filter is sometimes preferred to a linear filter because it may models the characteristics of natural phenomena more closely, thereby, resulting in superior performance compared to that of a linear filter. A nonlinear filter also performs better when the input signal is contaminated by non-additive and correlated noise.

However, linear filters are still the primary tool in many areas of signal and image processing largely due to their mathematical simplicity and ease of design and implementation. Another important reason for widespread use of linear filters is that many non-linear operations can be approximated by a combination of linear operations with an adequate level of accuracy and performance.

Both linear and nonlinear filters can be alternatively categorized, as adaptive or non-adaptive filters. A non-adaptive filter is used for a stationary input signal, resulting in an optimum performance in the mean-square sense. This is commonly known as the Wiener filter. However, the Wiener filter is inadequate for dealing with situations in which the signal is not stationary. In such situations, the optimum filter has to be time-varying, where the coefficients of the filter adapt in time to track the changes in the signal characteristics. Such filters are called adaptive filters.

Adaptive linear filters have been widely applied in diverse fields such as communications, radar, sonar, seismology, biomedical engineering and nondestructive testing. Layered earth modeling, channel equalization, linear predictive coding, echo cancellation, noise cancellation are some of the important applications of adaptive filters.

Adaptive linear filters can be further classified in terms of length of the impulse response as finite-length impulse response (FIR) filters and infinite-length impulse response (IIR) filters. The main feature that distinguishes an IIR filter from an FIR filter is the presence of feedback paths, which makes the duration of the impulse response infinitely long.

IIR filters generally require considerably fewer coefficients than the corresponding FIR filters, to achieve a given level of performance. For example, since the output feedback or auto-regressive (AR) part generates an infinitely long impulse response, IIR filters have very sharp spectral cut-off characteristic in contrast to the corresponding FIR filters.

Even though an adaptive IIR filter offers better performance than an adaptive FIR

filter having the same number of filter coefficients (feed-forward and feedback taps), it finds limited application largely due to problems inherent in IIR filter design such as local minima convergence and instability of operation during adaptation. Recent progress in the study of adaptive IIR filtering techniques has focused on the development of solutions to these two drawbacks.

Fundamentally, there have been two approaches to adaptive IIR filtering depending on formulations of the prediction error, namely the output error method [1] [2] and the equation error method [3].

Some of the existing filtering algorithms based on mean-square output error minimization are the finite memory recursive LMS [4] [5] and *a posteriori* LMS [6] algorithms. The major drawback of these methods is the convergence to a local minimum depending on initial conditions. In the output error minimization method, the problem of the local minima convergence occurs because the mean-square error surface of filter coefficients is non-quadratic [7].

The equation error method was proposed as a solution to the problem of local minima convergence prevalent in the output-error method. However, this method leads to biased estimates of the filter coefficients [8]. Furthermore, the equation-error formulation can be considered as a variation of adaptive FIR filtering since there is no contribution from the feedback of the filter output in defining the error function [9] [10].

It has been shown that the problem of convergence to a local minima can be solved under certain conditions particularly for the case of over- or exact modeling, i.e., when the order of the filter is chosen to be equal to or greater than that of the unknown signal or system [6] [11]. However, in the real world, the order of the signal is not known and it can be greater than the order of the chosen filter. This is the case of under-modeling which is more common in practice.

Another major problem associated with IIR filtering is that the poles of the filter may move outside the unit circle during adaptive processing, resulting in instability [6] [9]

[12]. Techniques for stability monitoring are therefore a subject of significant research interest. Another approach used for overcoming the instability problem is the use of alternate filter structures such as the cascade, parallel and lattice forms.

Lattice filters represent a substitute for direct implementation of the filtering operation preventing the instability problem. Many variations of the structure of lattice adaptive filters have been proposed that show considerable promise. However, in spite of these development, further research is required to be done towards solving these problems using more advanced techniques or improving the techniques in terms of reducing computational complexity.

Objective of Study

This research concentrates on the development of the theoretical basis and the practical implementation of a new adaptive IIR filtering algorithm for solving the local minima convergence problem in the output-error method. This technique is based on the homotopy continuation method for finding all roots of the output error function. The global minimum is then determined as the root associated with the minimum error.

It is shown that an appropriate modification of the homotopy continuation method is required in order to utilize the method in adaptive filtering applications. The development of a stable and globally converging algorithm based on the modification is the major focus of the initial part of this study. Problems encountered in the proposed approach are discussed, and further modifications in the structure of the filtering algorithm are introduced. Additional parameters are incorporated for controlling the convergence performance. The effects of these parameters on the filter performance are also evaluated.

The validation of the proposed algorithm through simulations is an important part of the study. In order to support the simulation results, and test the algorithm on a

practical problem, a real world application in noise cancellation is considered. Issues of stability in adaptive IIR filtering are also considered in the development of the basic algorithm and its variations.

Dissertation Summary

A review of various adaptive filtering techniques and recent developments are surveyed in Chapter 2. Especially, important issues in adaptive IIR filtering and the motivations for the recent research are stated. The nonlinearity in optimizing the filter coefficients in adaptive IIR filtering is discussed in detail. Advantages and disadvantages of existing adaptive IIR filtering techniques are also briefly summarized.

Chapter 3 presents the theory of the homotopy continuation method. A definition of the homotopy continuation method and relevant theory is discussed. Basic operations of the homotopy continuation method to solve nonlinear equations, namely prediction and correction, as well as its variations for improved solution tracking performance are described. The properties of solution paths, when a target system can be formulated with a set of polynomials, are also discussed in detail.

In Chapter 4, a new adaptive IIR filtering algorithm based on the homotopy continuation method is proposed. The adaptive IIR filtering is formulated as an iterative process for solving nonlinear polynomials with time-varying coefficients. The algorithm is derived by a suitable modification of the conventional homotopy continuation method. Parameters controlling the trade-off between convergence speed and system complexity are analyzed. Modifications in the filter structure for overcoming some of the inherent problems are also described.

Simulation results of the proposed algorithm and its variations are discussed in Chapter 5. Comparisons of the results with the performance of other algorithms are also given in this chapter.

In Chapter 6, for the purpose of further validation, the proposed algorithm is applied to a noise cancellation problem using real data. The algorithm is shown to be successfully in reducing interfering noise in ultrasonic nondestructive inspection signals.

Finally, conclusions of this study and further extension of this research for improvement of the algorithm are discussed in Chapter 7.

2 ADAPTIVE IIR FILTERING

Background

As mentioned in Chapter 1, adaptive filters can be categorized into linear filters and nonlinear adaptive filters, depending on the operator defining the input-to-output mapping. The filter can also be classified into analog and digital filters depending on the nature of signals. A digital filter offers comparable performance to that of an analog filter as long as the signal to be processed is sampled satisfying the sampling theorem. A digital adaptive filter can have a finite-length impulse response (FIR) or an infinite-length impulse response (IIR). This thesis focuses on linear digital adaptive IIR filtering algorithms.

The basic formulation of adaptive filtering can be stated as follows: Given an input signal and a desired response, an error or cost function is estimated by comparing the desired response and filter output. The estimated error function is then minimized with respect to the filter coefficients resulting in an iterative equation for updating the filter coefficients.

While maintaining the basic concept, different configurations of adaptive filtering, employed according to specific applications, differ in how and where the desired signal and filter output are extracted. Haykin [12] classifies applications of adaptive filtering into four classes. Different configurations of filtering are required in each application.

- Identification: system identification, layered earth modeling

- Inverse modeling: predictive deconvolution, adaptive equalization
- Prediction: linear predictive coding, adaptive differential pulse-code modulation, autoregressive spectrum analysis, signal detection
- Interference canceling: adaptive noise cancellation, echo cancellation, radar polarimetry, adaptive beamforming

Of the various applications mentioned above, system identification and adaptive noise cancellation are described in more detail. These two applications differ in the manner in which the desired signal and filter output signal are extracted. These applications are used later in the development of a new adaptive filtering algorithm.

System Identification

System identification is the estimation of the parameters of an unknown plant when the plant is modeled using a system (filter) represented by a set of delay elements and adjustable parameters. As shown in Figure 2.1, the input signal $u(n)$ of the unknown plant $V(z)$ is observed simultaneously by an adaptive filter $W(z)$. The plant output $d(n)$ serves as the purpose of a desired response of the filter output $y(n)$. The difference between $d(n)$ and $y(n)$ is the error $e(n)$.

The filtering algorithm is an iterative process to adjust the parameter of the filter to minimize $e(n)$. The iteration continues until the error becomes sufficiently small in some sense, usually in the sense of mean square measurement. The filter is considered to model the unknown plant successfully when the mean squared error is minimized. When the plant is time-varying, i.e., the plant output is nonstationary, the adaptive filtering algorithm has the task of not only keeping the modeling error minimized but also continually tracking the time variations in the dynamics of the plant.

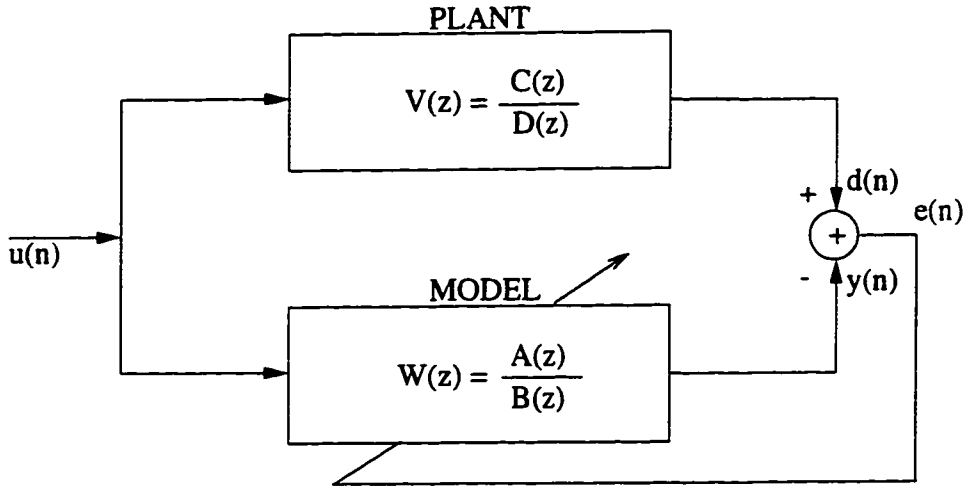

. Figure 2.1 System identification configuration

Adaptive Noise Cancellation

Adaptive filters for noise cancellation operate in a dual-input, closed-loop adaptive control system [12] [13] as shown in Figure 2.2. The inputs of the system are the primary and reference input signals. The primary input signal contains an information-bearing signal corrupted by additive noise expressed as

$$d(n) = s(n) + n_d(n) \tag{2.1}$$

The information-bearing signal $s(n)$ and the noise $n_d(n)$ are assumed to be uncorrelated.

The reference signal $u(n)$ contains only noise $n_r(n)$ that is assumed to be uncorrelated with $s(n)$ but correlated with $n_d(n)$. As illustrated in Figure 2.2, the same noise source is assumed to be present in both the primary and reference input signals.

The filter output $y(n)$ is subtracted from the $d(n)$, forming an error signal $e(n)$.

$$e(n) = d(n) - y(n) = s(n) + n_d(n) - y(n) \tag{2.2}$$

The adaptive filter $W(z)$ attempts to minimize the mean square of the error signal. The information-bearing component $s(n)$ is unaffected by the filtering since it is uncorrelated with either $n_d(n)$ or $u(n)$.

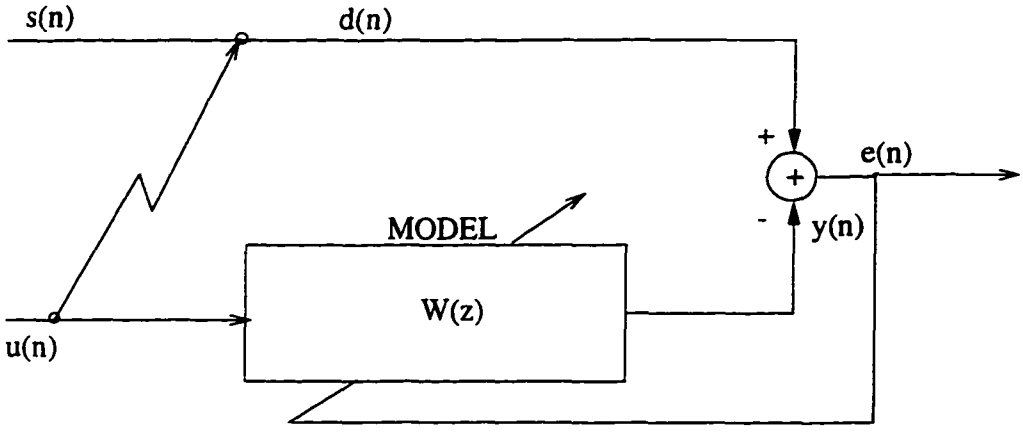

Figure 2.2 Adaptive noise cancellation configuration

There are two limiting cases in the filtering operation [12]:

1. The noise filtering operation is perfect in the sense that $y(n) = n_d(n)$. In this case, the system output $e(n)$ is noise-free and perfect noise cancellation is achieved.

2. The reference signal is completely uncorrelated with both the signal and noise component of the primary input signal $d(n)$. In this case the adaptive filter switches itself off resulting in a zero value of the output $y(n)$. Hence the system output $e(n)$ is the same as $d(n)$.

The underlying concept of the second limiting case is utilized in adaptive grain noise cancellation in Chapter 6.

Adaptive IIR Filtering

An adaptive IIR filter is usually preferred to an adaptive FIR filter with the same number of filter coefficients largely due to the fact that it can provide significantly better performance. Fundamentally, there have been two approaches to adaptive IIR filtering, corresponding to different formulations of the prediction error, known as equation error

and output error methods. In the equation error approach, the feedback coefficients of an IIR filter are updated in a nonrecursive form [8]. This formulation is essentially a type of adaptive FIR filtering and resulting in biased estimates of filter coefficients. In the adaptive IIR filtering based on output error minimization approach [14] [15], it is known that the error surface is not quadratic and, hence, the estimated filter coefficients may converge to values of local minima.

Efforts to solve the main drawbacks, namely local minimum convergence and biased estimation, have been two main branches of study in adaptive IIR filtering. Since the equation error minimization approach is closely related to adaptive FIR filtering rather than adaptive IIR filtering, the main focus of this dissertation is on adaptive IIR filters employing the output error minimization approach.

In order to understand the local minimum convergence problem in an adaptive IIR filter using the output error minimization approach, the structure of the IIR filter is analyzed in terms of its nonlinearity. After introducing the basic form of adaptive IIR filtering algorithm based on the output error minimization approach, the structure of adaptive IIR filters employing an equation error formulation is explained and contrasted. Instability problems inherent to IIR filters are also discussed as another important consideration in the development of adaptive IIR filtering algorithms.

IIR Filter

The auto-regressive and moving average (ARMA) filter $W(z)$ shown in Figure 2.3, can be expressed, in the frequency domain, in a rational form using feed-forward coefficients, $\alpha(n)$, feedback coefficients, $\beta(n)$, and delay elements as

$$W(z) = \frac{\alpha_0(n) + \alpha_1(n)z^{-1} + ... + \alpha_p(n)z^{-p}}{1 - \beta_1(n)z^{-1} - ... - \beta_q(n)z^{-q}} \equiv \frac{A(z)}{B(z)} \ , p < q \tag{2.3}$$

In time domain, $w(n) = Z^{-1}[W(z)]$ is expressed as an infinite-length impulse response (IIR).

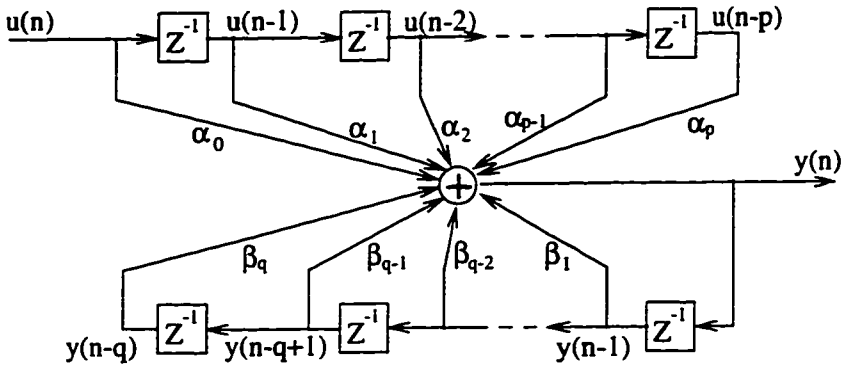

Figure 2.3 IIR filter: ARMA model

Assuming the filter and input signal to be causal, the filter output signal, $y(n)$, is expressed as,

$$y(n) = \sum_{i=0}^{\infty} w(i)u(n-i) = \sum_{i=0}^{p} \alpha_i(n)u(n-i) + \sum_{j=1}^{q} \beta_j(n)y(n-j) \tag{2.4}$$

The output signal $y(n)$ can be expressed by the inner product

$$y(n) = \vec{\theta}(n)^T \vec{\phi}(n) \tag{2.5}$$

where

$$\vec{\theta}(n) = [\alpha_0(n)\ \alpha_1(n)\ ...\ \alpha_p(n)\ \beta_1(n)\ \beta_2(n)\ ...\beta_q(n)]^T \tag{2.6}$$

$$\vec{\phi}(n) = [u(n)\ ...\ u(n-p+1)\ y(n-1)\ ...\ y(n-q)]^T \tag{2.7}$$

The output signal $y(n)$ is clearly a nonlinear function of $\vec{\theta}(n)$ because the delayed output signals $y(n-j)$ in $\vec{\phi}(n)$ depend on the previous filter coefficients and filter output values [9].

Output Error Minimization Approach

In the output error minimization approach, the cost function to be minimized is defined as mean squared output error (MSOE), ξ, between filter output $y(n)$ and the

desired signal $d(n)$. In the least mean square (LMS) based algorithms, the objective of adaptive filtering can be stated as

$$\min_{\vec{\theta}} E[e^2(n)] = \min_{\vec{\theta}} E[(d(n) - y(n))^2] \tag{2.8}$$

Since the filter output $y(n)$ is a nonlinear function of filter coefficients, the output error, $e(n)$, is also a nonlinear function of the coefficients $\vec{\theta}(n)$. Therefore, the mean squared error (MSE) ξ is not a quadratic function and can have multiple local minima [7].

In adaptive IIR filtering, the true mean of squared error is not available but only an instantaneous estimate of the MSE is observable at every iteration step n, expressed by

$$e(n) = d(n) - y(n) = d(n) - \vec{\theta}(n)^T \vec{\phi}(n) \tag{2.9}$$

In conventional gradient descent adaptive filtering algorithms, the filter coefficients are updated according to the gradient of the squared error function based on the steepest descent method:

$$\delta\vec{\theta}(n) = -\frac{1}{2}\eta \frac{d}{d\vec{\theta}(n)} e^2(n) \tag{2.10}$$

where η is a convergence constant. This leads to a filter coefficients updating algorithm expressed as [9] [10] [16]

$$\vec{\theta}(n) = \vec{\theta}(n-1) + \eta\vec{\phi}(n)[d(n) - \vec{\theta}(n)^T \vec{\phi}(n)] \tag{2.11}$$

The implication of Eq. (2.11) is that the algorithm needs to store all previous input signals to obtain $\vec{\phi}(n)$. In order to overcome the unlimited growing memory problem, many adaptive IIR filtering techniques based on the LMS approach such as finite memory recursive LMS [4] [5], a posteriori LMS and the extended LMS [6] using a finite number of previous data have been developed for calculating $y(n)$.

As mentioned before, all these methods based on the LMS approach have the problem of convergence to local minima. Extensive studies, addressing the issue of convergence to local minima, have proved that when the filter is under-modeled, i.e., the order of

either pole polynomial or zero polynomial is smaller than that of the unknown plant, the local minimum always exists [17] [18] [19].

When a filter has only feed-forward taps, i.e., an FIR filter, the MSE error surface is quadratic and has a single minimum [20]. This problem is therefore relatively easier to handle.

While the LMS based filtering algorithms are derived using the ensemble average, recursive least square (RLS) approach involves the use of time averages. Consider the system identification example shown in Figure 2.1. Suppose we have a set of measurements $u(1)$, $u(2)$, ..., u(M), made at times t_1, t_2, ..., t_M. In the RLS method, the error between filter output $y(n)$ and desired signal $d(n)$ is computed during the observation interval M, and minimized with respect to filter coefficients as

$$\min_{\vec{\theta}} \sum_{n=0}^{M-1} |e(n)|^2 = \min_{\vec{\theta}} \sum_{n=0}^{M-1} |(d(n) - y(n)|^2 \tag{2.12}$$

Then, the optimum value of filter coefficients is defined by

$$\hat{\vec{\theta}} = \Phi_{\phi\phi}^{-1} \Phi_{\phi d} \tag{2.13}$$

where the $\Phi_{\phi\phi}$ is a auto-correlation matrix of $\phi(n)$ and the $\Phi_{\phi d}$ is cross-correlation matrix of $\phi(n)$ and $d(n)$. The correlation functions are estimated using the M previous $\phi(n)$ and desired signals $d(n)$.

The RLS algorithm, which is not stated in detail here, is derived from the above relation for iteratively calculating the optimum filter coefficients. The correlation functions are recursively updated according to incoming signals. Since $\phi(n)$ is again a function of previous output $\phi(n-1)$, $\phi(n-2)$, ... $\phi(n-M+1)$, the problem of local minima convergence still exists in the RLS approach.

Equation Error Minimization Approach

A filter structure using equation-error minimization approach was suggested [3], to solve the local minimum convergence problem of the output-error minimization ap-

proach.

In order to avoid the non-quadratic behavior of the error surface of the output error minimization approach, in the equation-error minimization approach, the feedback from the filter output signal is replaced with that of the desired signal, as illustrated in Figure 2.4, assuming the filter output $y(n)$ is close to desired signal [5].

The filter output of the equation-error method is characterized by a non-recursive difference equation as

$$y_e(n) = \sum_{m=1}^{q} \beta_m(n) d(n-m) + \sum_{m=0}^{p} \alpha_m(n) u(n-m) \tag{2.14}$$

where $(\beta_m(n), \alpha_m(n))$ are the filter coefficients.

The delay-and-sum operators $A(z)$ and $B(z)$ appearing in the figure are expressed as

$$A(z) = \sum_{m=0}^{p} \alpha_m(n) z^{-m} = Z^{-1}[a(n)] \tag{2.15}$$

$$B(z) = \sum_{m=1}^{q} \beta_m(n) z^{-m} = Z^{-1}[b(n)] \tag{2.16}$$

Notice that the filter output does not depend on its delayed samples, i.e., the filter does not have a feedback.

The error $e(n)$ is called an equation error since it is generated by subtracting two difference equations as

$$\begin{aligned} e(n) &= d(n) - y_e(n) && \text{(2.17a)} \\ &= d(n) - [b(n) * d(n) + a(n) * u(n)] && \text{(2.17b)} \\ &= [d(n) - b(n) * d(n)] - [a(n) * u(n)] && \text{(2.17c)} \end{aligned}$$

Since there is no feedback from the filter output $y_e(n)$, the equation error is a linear function of the coefficients, hence the MSE is a quadratic function with a single global minimum and no local minima [21]. In many ways, the equation-error adaptive filter functions like an adaptive FIR filter and possesses similar convergence properties. The

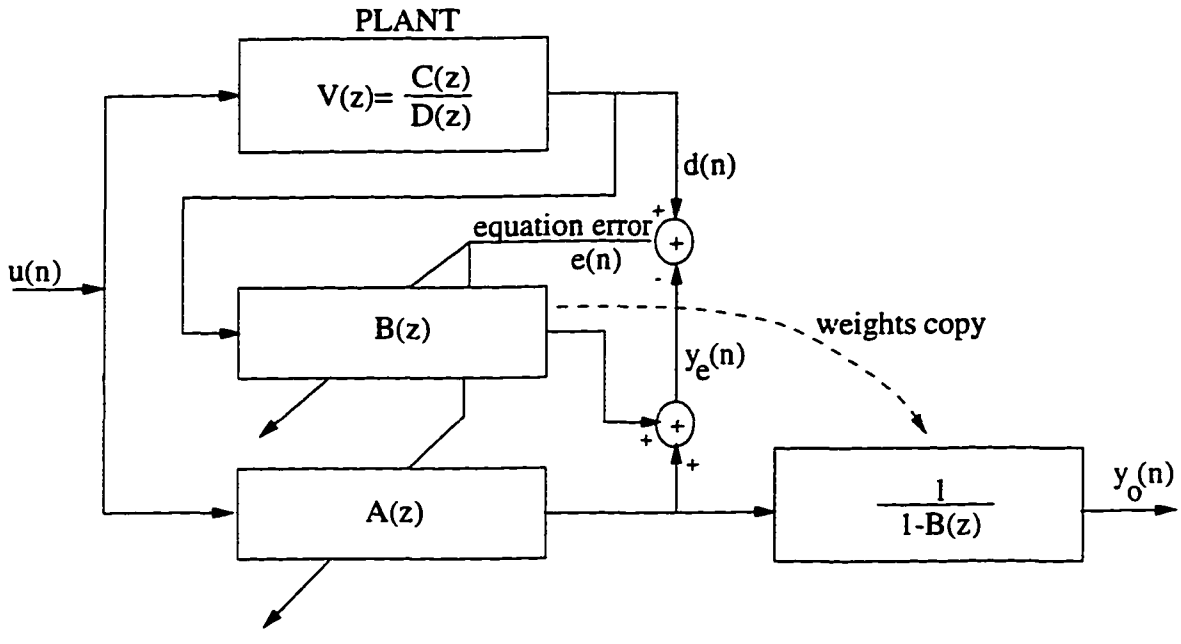

Figure 2.4 Equation error minimization formulation

main difference is that the equation-error adaptive IIR filter can operate as an ARMA model by copying and inverting the $(1 - B(z))$ term, as shown in Figure 2.4.

The drawback of this approach is that if the desired signal $d(n)$ is very noisy, then a severe bias is introduced into the filter output $y(n)$ [5] [9].

Instability Problem

One of major drawbacks associated with the conventional adaptive IIR filtering algorithms, represented by the basic filter coefficient update algorithm shown in Eq. (2.11), is the instability problem. When a zero of the pole polynomial of the filter accidentally updates and stays outside the unit circle for a significant length of time, the filter output can grow unbounded. To prevent this behavior, some form of stability monitoring is required.

Some of the earliest studies in the stability monitoring consist of testing whether

any pole is outside the unit circle [22] [23]. However, these methods require additional factorization to determine which pole is outside the unit circle, which is usually computationally expensive when the pole polynomial is of a high degree. Recent studies have shown alternative realizations such as parallel and lattice structures can solve the instability problem. The parallel form consists of a second-order filter unit in which the factorization is trivial and the lattice structure requires each reflection coefficient to be less than unity [9].

Review of Recent Work

Recent studies in adaptive IIR filtering algorithms have focused on three major directions: development of (i) new algorithms using an output error minimization approach, (ii) new algorithms using equation error minimization approach, and (iii) algorithms without the instability problem. In this section, some recent studies on the development of new algorithms based on output error minimization approach and its applications, and efforts to overcome the instability problem are summarized.

The Steiglitz-Mcbride adaptive IIR filtering algorithm [24] is one of the well-known methods to solve the local minimum convergence problem. In this method, a composite error surface defined by output error and equation error jointly is used in the gradient search of the global minimum. However, this method does not always guarantee the global minimum convergence when the filter converges to any local minimum located far from the global minimum.

Another algorithm proposed by Kenney and Rohrs [25] considers a dynamic composite error surface. In this algorithm, the property of error surface can be changed from an equation error surface and an output error surface depending on a composition parameter. An algorithm called a composite gradient algorithm proposed by Simon and Peceli [26] uses a similar approach. Both algorithms still do not always guarantee

global minimum convergence, and the performance of the algorithms largely depends on a proper selection of the composition parameter.

An alternative IIR filter structure proposed by Crawford [27] uses a so-called full-feedback configuration to enhance the convergence rate, but it ignores the local minimum convergence problem.

Structural variation is a widespread approach for solving the instability problem. Parallel [28], cascade [29] and lattice structures have been proposed as alternative structures of direct form adaptive IIR filters. Especially, intensive studies on the algorithms using the lattice structure have yielded many effective algorithms [30] [31] [32] [33] [34]. Use of genetic algorithm has been proposed as an alternative low complexity approach to solve the instability problem [35].

The superiority of adaptive IIR filters over FIR filters have been proved in recent studies of various applications such as time delay estimation [36], echo cancellation [37], adaptive line enhancement [38] and adaptive noise control [39]. These algorithms focus on the effectiveness of quick response to time-varying signal and stability.

3 HOMOTOPY CONTINUATION METHOD

The homotopy continuation method (HCM) is a numerical method for calculating all solutions of a (set of) nonlinear equation(s). The HCM has been used in many applications in a variety of disciplines including Chemical [44], Power [45], Linear programming [46] [47] and Electrical Engineering [48] [49].

The underlying concept of the method involves identifying a simple equation with known solutions and slowly deforming it into a desired equation with unknown solutions. During the deformation process, a family of paths is defined from the known solutions of the simple equation to the desired solutions of the given equation. The continuation method is a numerical procedure used to track the solution paths [50] [51].

Unlike the gradient based numerical methods such as the Newton method [52] [53], the HCM is globally convergent and solution exhaustive. Globally convergent implies that the method will converge to a solution from any initial starting point. Solution exhaustive means that all solutions to the desired equation can be found. One merit of the HCM is that it finds solutions of nonlinear polynomials in an iterative way in contrast to other nonlinear polynomial solution methods such as the Bairstow's method [54] in which roots of polynomials are found noniteratively by systematic division and multivariate Newton method.

Definition of Homotopy Function

The homotopy function is defined as follows [52] [55].

Definition: Two continuation maps, g, $f: X \to Y$ are said to be homotopic if g can be continuously deformed into f, that is, there exists a continuous family of maps $h_\tau: X \to Y$, $(0 \leq \tau \leq 1)$, such that $h_0 = g$ and $h_1 = f$. Define

$$h(x, \tau) = h_\tau(x) \quad (x \in X, \ \tau \in I) \tag{3.1}$$

where I is the unit interval, such that $h(x, 0) = g(x)$ and $h(x, 1) = f(x)$ for all $x \in X$.

The map h is continuous with respect to τ as well as x. The map h is referred to as a homotopy function between $g(x)$ and $f(x)$ and is represented as

$$h: \ g \approx f \tag{3.2}$$

In the homotopy continuation method, a simple system of equations with known solutions is continuously deformed into a target system of equations as illustrated in Figure 3.1. As the equations are deformed ($\tau \to 1$), the solutions of the starting equations approach the solutions of the target equation. A most frequently used homotopy function called an "all-solution homotopy" is expressed as

$$h(x, \tau) \equiv (1 - \tau)g(x) + \tau f(x) = 0 \tag{3.3}$$

Here, $f(x)$ refers to the target equation and $g(x)$ is the starting equation with known solutions. The parameter τ plays a role of an indexing variable from $g(x)$ to $f(x)$ such that at $\tau = 0$, $h(x, 0) = g(x)$ and $h(x, 1) = f(x)$ when $\tau = 1$. As the homotopy parameter τ varies from 0 to 1, the solutions to the homotopy equation trace out a path in the parameter space from the known solution to the desired solution of $f(x) = 0$. A well-known method to track the solution path is 'prediction and correction method'. The details of this method is described later in this chapter.

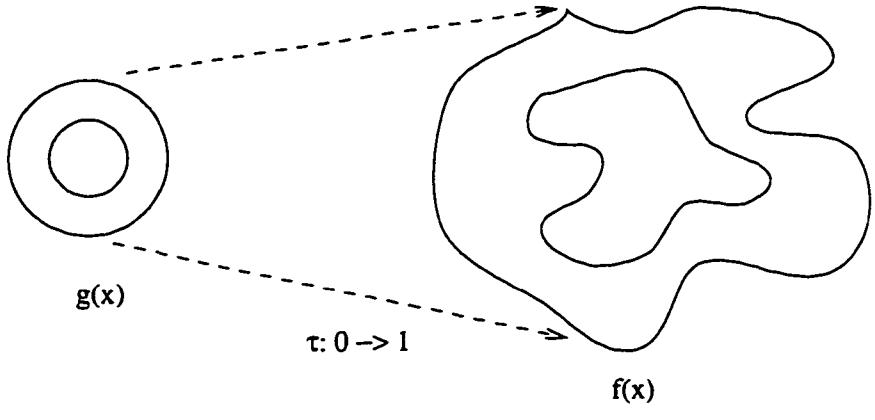

Figure 3.1 Homotopy mapping

Path Existence and Regularity

The application of homotopy continuation method requires the existence of solution paths. There are several examples of non-paths such as crossings, isolated points, spirals and bifurcations [55]. The existence of paths require that the homotopy function defined by Eq. (3.3) consist of differentiable curves. This condition has been presented and proved in [56].

Given a homotopy function $H : R^{n+1} \rightarrow R^n$, define

$$H^o = \{(\vec{x}, \tau) \| H(\vec{x}, \tau) = 0\} \tag{3.4}$$

as the set of all solutions $(\vec{x}, \tau) \in R^{n+1}$ to the system $H(\vec{x}, \tau) = 0$, where

$$\vec{x} = [x_1 \; x_2 \ldots \; x_n]^T. \tag{3.5}$$

The Jacobian of the homotopy function can be written as

$$H'(\vec{x}, \tau) = \begin{bmatrix} \frac{\partial h_1}{\partial x_1} & \cdots & \frac{\partial h_1}{\partial x_n} & \frac{\partial h_1}{\partial \tau} \\ & & \cdots & \\ \frac{\partial h_n}{\partial x_1} & \cdots & \frac{\partial h_n}{\partial x_n} & \frac{\partial h_n}{\partial \tau} \end{bmatrix} \tag{3.6}$$

Define an augmented vector $\vec{u} = [\vec{x}\ \tau]^T$ of size $(n+1) \times 1$ so that $u_i = x_i, i = 1, \ldots n$ and $u_{n+1} = \tau$, where $\vec{x} \in R^n, \vec{u} \in R^{n+1}$.

Then, the Jacobian $H'_{-i}(\vec{u})$ is an $n \times n$ matrix with ith column removed.

$$H'_{-i}(\vec{u}) = \begin{bmatrix} \frac{\partial h_1}{\partial u_1} \cdots & \frac{\partial h_1}{\partial u_{i-1}} \frac{\partial h_1}{\partial u_{i+1}} & \cdots \frac{\partial h_1}{\partial u_{n+1}} \\ & \cdots & \\ \frac{\partial h_n}{\partial u_1} \cdots & \frac{\partial h_n}{\partial u_{i-1}} \frac{\partial h_n}{\partial u_{i+1}} & \cdots \frac{\partial h_n}{\partial u_{n+1}} \end{bmatrix} \tag{3.7}$$

It has been proved that there exists a single continuously differential path for $(\vec{x}, \tau) \in H^o$, if the matrix $H'_{-i}(\vec{u})$ is nonsingular [56].

Path Description: Path Tracking Methods

A solution path, or a path, is defined as a differentiable curve consisting of points $(\vec{x}, \tau)$ satisfying $H(\vec{x}, \tau) = 0$.

There exist many known path tracking algorithms [57], the most common one being the prediction-correction (PC) method.

Given a function $f(x)$ of an unknown variable x, the homotopy function to solve $f(x) = 0$ is rewritten from Eq. (3.3)

$$h(x, \tau) = (1 - \tau)g(x) + \tau f(x) \tag{3.8}$$

where $g(x)$ is a starting function with known solutions, which is homotopic to the target function $f(x)$.

The solutions to $h(x, \tau) = 0$ can be tracked starting from the known solutions of $g(x) = 0$ to the solutions of $f(x) = 0$ by incrementing the τ from 0 to 1. A widely used path tracking method called a prediction-correction method is an iterative procedure consisting of two steps:

1. Prediction of the next solution to $h(x, \tau) = 0$, corresponding to the increased τ by a small increment $\Delta\tau$.

2. Correction to the true solution from the prediction

In order to prevent a large deviation from the path, a small value is chosen for the increment $\Delta\tau$ in the prediction step. When $f(x) = 0$ has multiple solutions, each solution path is required to be tracked separately.

Suppose the equation $h(x, \tau) = 0$ has d paths and τ is monotonically increasing with respect to the length of paths. The detail of the prediction-correction path tracking procedure for finding the jth solution ($1 \leq j \leq d$), illustrated in Figure 3.2, is as follows:

1. *Prediction: at the iteration step n, the next position* $(x_j^*(n+1), \tau(n+1) = \tau(n)+\Delta\tau)$ *is predicted from the current position* $(x_j(n), \tau(n))$ *in the direction of increment of* τ *by* $\Delta\tau$.

2. *Correction: the predicted value* $(x_j^*(n+1), \tau(n+1))$ *is corrected to closest position* $(x_j(n+1), \tau(n+1))$ *to satisfy* $h(x_j(n+1), \tau(n+1)) = 0$, *($\tau$ is fixed during the correction), using any nonlinear function solution method such as the Newton method.*

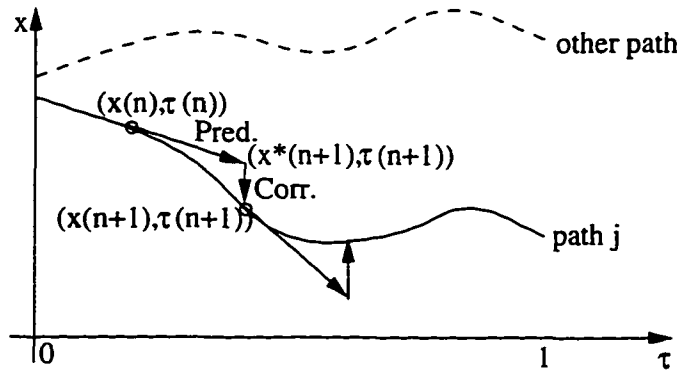

Figure 3.2 The prediction and correction step for path tracking in HCM

Prediction Step

In the prediction step, the amount of change in the unknown variable x, say Δx, corresponding to the increment $\Delta\tau$ is required to be calculated at every iteration step. There are two well-known approaches to calculate Δx: a prediction based on homotopy differential equation (HDE prediction) and a prediction based on the basic differential equation (BDE prediction). The HDE prediction method is used when τ increases as the length of a path increases. The BDE prediction method has been developed for the case that τ may decrease with respect to the path length. These approaches are described in more detail, below.

1. HDE Prediction

Since a homotopy function is equal to 0 along the path, the derivative of the homotopy function with respect to the homotopy parameters τ is also equal to 0 at any position on the path. The procedure for calculating the change in the unknown variable, Δx, with respect to a corresponding increment $\Delta\tau$ is obtained from the derivative of the homotopy function.

Consider the homotopy function from Eq. (3.3)

$$h(x,\tau) = (1-\tau)g(x) + \tau f(x) \tag{3.9}$$

where a target equation $f(x)$ has an unknown variable x. The homotopy function $h(x,\tau)$ of two variables x and τ, can be expressed as a function of τ as

$$h(x,\tau) = h(u(\tau),\tau) = h(u(\tau),v(\tau)) \tag{3.10}$$

by defining $x \equiv u(\tau)$ and $\tau \equiv v(\tau)$.

Using the chain rule, the derivative of homotopy function with respect to τ is

$$\begin{aligned} \frac{d}{d\tau}h(u(\tau),v(\tau)) &= \frac{\partial}{\partial u}h(u(\tau),v(\tau))\frac{d}{d\tau}u(\tau) + \frac{\partial}{\partial v}h(u(\tau),v(\tau))\frac{d}{d\tau}v(\tau) \\ &= \frac{\partial}{\partial x}h(x,\tau)\frac{dx}{d\tau} + \frac{\partial}{\partial \tau}h(x,\tau) = 0 \end{aligned} \tag{3.11}$$

so

$$\frac{dx}{d\tau} = -[\frac{\partial}{\partial x}h(x,\tau)]^{-1}\frac{\partial}{\partial \tau}h(x,\tau) \tag{3.12}$$

Therefore, the increment Δx corresponding to an increment $+\Delta\tau$ is calculated by

$$\Delta x = \frac{dx}{d\tau}\Delta\tau = -[\frac{\partial}{\partial x}h(x,\tau)]^{-1}\frac{\partial}{\partial \tau}h(x,\tau)\Delta\tau \tag{3.13}$$

This procedure can be easily extended to the case of a set of polynomials in multiple variables $\vec{x}$, where

$$\Delta\vec{x} = \frac{d\vec{x}}{d\tau}\Delta\tau = -[H'_{\vec{x}}(\vec{x},\tau)]^{-1}\frac{\partial}{\partial \tau}H(\vec{x},\tau)\Delta\tau \tag{3.14}$$

where $H'_{\vec{x}}(\vec{x},\tau)$ is the Jacobian matrix of the homotopy function $H(\vec{x},\tau)$ represented as

$$H(\vec{x},\tau) = [h_1(\vec{x},\tau)\ h_2(\vec{x},\tau)\ ...\ h_n(\vec{x},\tau)]^T \tag{3.15}$$

If τ is monotonically increasing as the length of the path increases, solving the above equation provides the required increment Δx for each $\Delta\tau$.

The stepsize $\Delta\tau$ decides how fast the path approaches the solution to $f(x) = 0$. However, a large value of $\Delta\tau$ may cause a path to deviate too far and, this may cause the path to converge to a point in a neighboring path in the correction step.

2. BDE Prediction

The HDE prediction method to calculate the increment $\vec{x}$ corresponding to a change in the homotopy parameter τ will fail to find a true solution on a path when τ is not monotonically increasing with the length of the path. Figure 3.3 shows the case, where the τ may decrease along increasing path length. When τ has to be decreased to satisfy $h(x,\tau) = 0$ on a path, a prediction by a positive increment $+\Delta\tau$ leads to an incorrect solution.

To overcome this difficulty, the path is parametrized in terms of path length, denoted by s, which is always increasing along the path. In this scheme, the homotopy parameter

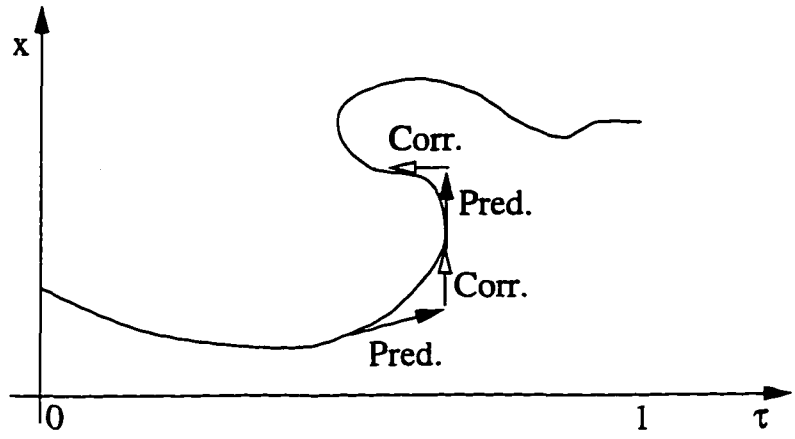

Figure 3.3 The prediction and correction step following path length

τ is considered as one of the unknown variables of the augmented vector which is varying along the path length s. That is, both x and τ are parameters guiding the prediction. In every iteration of prediction, the parameter with the largest slope in the previous iteration is selected as the path parameter. In the correction step, the value of the chosen parameter is fixed and the rest of variables are corrected using the Newton method or other nonlinear function solution methods.

The variables including τ are expressed as function of path length s.

$$\vec{x}(s) = [x_1(s)\ x_2(s) \ldots x_n(s)\ x_{n+1}(s)]^T \tag{3.16}$$

where $x_{n+1}(s) \equiv \tau$.

Let the parameter with the largest tangent be x_i. Then, the derivative of the path with respect to x_i has the following form.

$$\frac{d}{ds}\vec{x}(s) = [\frac{dx_1}{ds} \ldots \frac{dx_{i-1}}{ds}\ \ 1\ \ \frac{dx_{i+1}}{ds} \ldots \frac{dx_{n+1}}{ds}]^T \tag{3.17}$$

The increment of other variables corresponding to the increment $\Delta x_i(s)$ in $x_i(s)$ can be calculated in a similar manner used in the HDE prediction [55].

$$\Delta\vec{x}_{-i} = \Delta x_i \frac{d\vec{x}_{-i}}{dx_i} \tag{3.18a}$$

$$= \Delta x_i [H'_{\vec{x}}(\vec{x}(s))_{-i}]^{-1} \frac{\partial}{\partial x_i} H(\vec{x}(s)) \tag{3.18b}$$

where the subscript $(-i)$ means the ith element of the vector or ith column of the matrix has been deleted.

$$H'_{\vec{x}}(\vec{x}(s))_{-i} = \begin{bmatrix} \frac{\partial h_1(\vec{x})}{\partial x_1} \cdots & \frac{\partial h_1(\vec{x})}{\partial x_{i-1}} & \frac{\partial h_1(\vec{x})}{\partial x_{i+1}} & \cdots \frac{\partial h_1(\vec{x})}{\partial x_{n+1}} \\ & \cdots & & \\ \frac{\partial h_n(\vec{x})}{\partial x_1} \cdots & \frac{\partial h_n(\vec{x})}{\partial x_{i-1}} & \frac{\partial h_n(\vec{x})}{\partial x_{i+1}} & \cdots \frac{\partial h_n(\vec{x})}{\partial x_{n+1}} \end{bmatrix} \tag{3.19}$$

and

$$\frac{\partial}{\partial x_i} H(\vec{x}(s)) = [\frac{\partial h_1(\vec{x})}{\partial x_i} \cdots \frac{\partial h_{n-1}(\vec{x})}{\partial x_i} \frac{\partial h_n(\vec{x})}{\partial x_i}]^T \tag{3.20}$$

Since the prediction is along the direction of maximum slope, the distance to the corrected path is always minimum, in contrast to the HDE prediction method. This also reduces the risk of deviating from the true path and merging with a neighboring path. However, the calculation of the Jacobian is more complex operation than that of HDE prediction method.

There are other variations of the HDE and BDE prediction methods. For example, one of more preferred techniques is based on a procedure where the correction is performed to the closest point on the path [55]. That is, the parameter with the largest slope is not fixed any more and is also allowed to vary during the correction step. Since the convergence direction is normal to the path, the distance for correction is shortest, but the computational complexity is increased since the dimension of the Jacobian is increased by one.

Correction Step

The correction step can be performed using any nonlinear solution method. Some of commonly used nonlinear solution methods include bisection method, the Newton method, the Secant method and, fixed points and functional iteration method [52] [53].

One of most popular methods, the Newton method has been used in many existing applications of the homotopy continuation method.

Assuming τ is fixed, i.e., the HDE prediction is used, correction using Newton method is represented by the following iterative operation.

$$\vec{x}^{k+1} = \vec{x}^{k} - \frac{H(\vec{x}^{k}, \tau^{i})}{H'_{\vec{x}}(\vec{x}^{k}, \tau^{i})} \tag{3.21}$$

where

i: iteration number of prediction-correction step

τ^i: homotopy parameter at ith prediction-correction iteration
which is fixed during the correction

k: iteration number within a correction step

$H(\vec{x}^k, \tau^i)$: homotopy function evaluated at $(\vec{x}, \tau) = (\vec{x}^k, \tau^i)$

$H'_{\vec{x}}(\vec{x}^k, \tau^i)$: Jacobian of $H(\vec{x}, \tau)$ evaluated at $(\vec{x}, \tau) = (\vec{x}^k, \tau^i)$

$\vec{x}^k$: estimated solution during correction at the kth iteration

$\vec{x}^{k+1}$: estimated solution during correction at the $(k+1)$th iteration

Note that i is the iteration number for path tracking. Each iteration consists of a prediction step and a correction step. For a fixed value τ^i, the correction is performed by an inner-loop iteration. A similar iterative operation can be easily derived when the prediction is performed by the BDE prediction method.

Path Characteristics of Polynomial Systems

Consider a system $F(\vec{x})$ representing a set of polynomials. Then, the homotopy function is written as

$$H(\vec{x}, \tau) = (1 - \tau)G(\vec{x}) + \tau F(\vec{x}) = 0 \tag{3.22}$$

where

$$\vec{x} \;=\; [x_1 \; x_2 \; \ldots \; x_n]^T \tag{3.23a}$$

$$H(\vec{x},\tau) = [h_1(\vec{x},\tau)\ h_2(\vec{x},\tau)\ ...\ h_n(\vec{x},\tau)]^T \quad (3.23b)$$

$$G(\vec{x}) = [g_1(\vec{x})\ g_2(\vec{x})\ ...\ g_n(\vec{x})]^T \quad (3.23c)$$

$$F(\vec{x}) = [f_1(\vec{x})\ f_2(\vec{x})\ ...\ f_n(\vec{x})]^T \quad (3.23d)$$

and each $g_i, i = 1, ..., n$, corresponding to each $f_i, i = 1, ..., n$, is chosen to be

$$g_i(\vec{x}) = p_i^{d_i} x_i^{d_i} - q_i^{d_i},\ i = 1, ..., n \quad (3.24)$$

Here, n is the number of unknown variables and, equivalently, the number of given polynomials. The complex values p_i and q_i are chosen independent of the coefficients of polynomials and d_i is the order of the polynomial i. An example showing the procedure for the "independent" selection of p_i and q_i is presented in Appendix.

The number of solutions for an n-polynomials system with n unknown complex variables is well analyzed in [58]. When the target equations $F(\vec{x})$ are a set of polynomials in complex variables, it is very important to understand the path behavior and characteristics before we apply the HCM.

Path Characteristics

Morgan [55] has proved an important result for defining path characteristics of polynomials systems in complex variables.

Theorem: For a system of n polynomials, defined as Eq. (3.22), of degree $d_1, d_2, ... d_n$,

- The solution set $\{(\vec{x},\tau) \in C^n \times [0,1) : H(\vec{x},\tau) = 0\}$ is a collection of d nonoverlapping and smooth paths, where d is a total degree of $F(\vec{x})$ expressed as $d = d_1 \times d_2 \times ... \times d_n$.
- The paths move from $\tau = 0$ to $\tau = 1$ without backtracking in τ [59].
- Each geometrically isolated solution of $F = \vec{0}$ of multiplicity m has exactly m continuation paths converging to it.

- A continuation path can diverge to infinity only as $\tau \rightarrow 1$.
- If $F = \vec{0}$ has no solution at infinity, all the paths remain bounded. If $F = \vec{0}$ has a solution at infinity, at least one path will diverge to infinity as $\tau \rightarrow 1$ according to the Bezout theorem [55][60]. Each geometrically isolated solution at infinity of $F = \vec{0}$ of multiplicity m will generate exactly m diverging continuation paths.

Consequently, of all the possible cases shown in Figure 3.4, there are only three possible path behaviors namely (a) bounded and non-overlapped paths, (b) paths with multiplicity and (c) diverging paths. The theory defining the path property of a polynomial system helps in the application of homotopy continuation method to adaptive filtering. The problem of adaptive filtering formulated using a set of polynomials has the following properties.

- There is no path crossing (as shown at Figure 3.4 (e)) or non-path behavior (as shown in Figure 3.4 (f)) for a polynomials system. Path merging (as shown in Figure 3.4 (d)) can be controlled easily, for instance, by factorization.
- A diverging path results in a pole outside unit circle, which is not useful in adaptive filtering since this will lead to instability of the filter.
- Multiplicity of paths will not cause any problem in adaptive filtering based on the HCM since the final solution chosen is the one associated with the minimum error.
- Since there is no backtracking in terms of τ, the prediction based on BDE is not necessarily used. Since the BDE prediction requires calculation of the Jacobian with one additional variable, the prediction-correction based on HDE is preferred. However, the BDE prediction is closer to a path than HDE prediction, resulting in faster convergence speed at the correction step.

- One problem that is still prevalent in path tracking is path merging. To avoid the path merging, polynomials can be factorized after each root is computed. In adaptive filtering applications, the possibility of path merging can be higher since the polynomials have time-varying coefficients. The stepsize in τ or path length must be deliberately chosen to avoid frequent occurrence of path merging. It is shown later that parameters of the algorithm that control the convergence rate can be chosen such that the possibility of path merging is minimized.

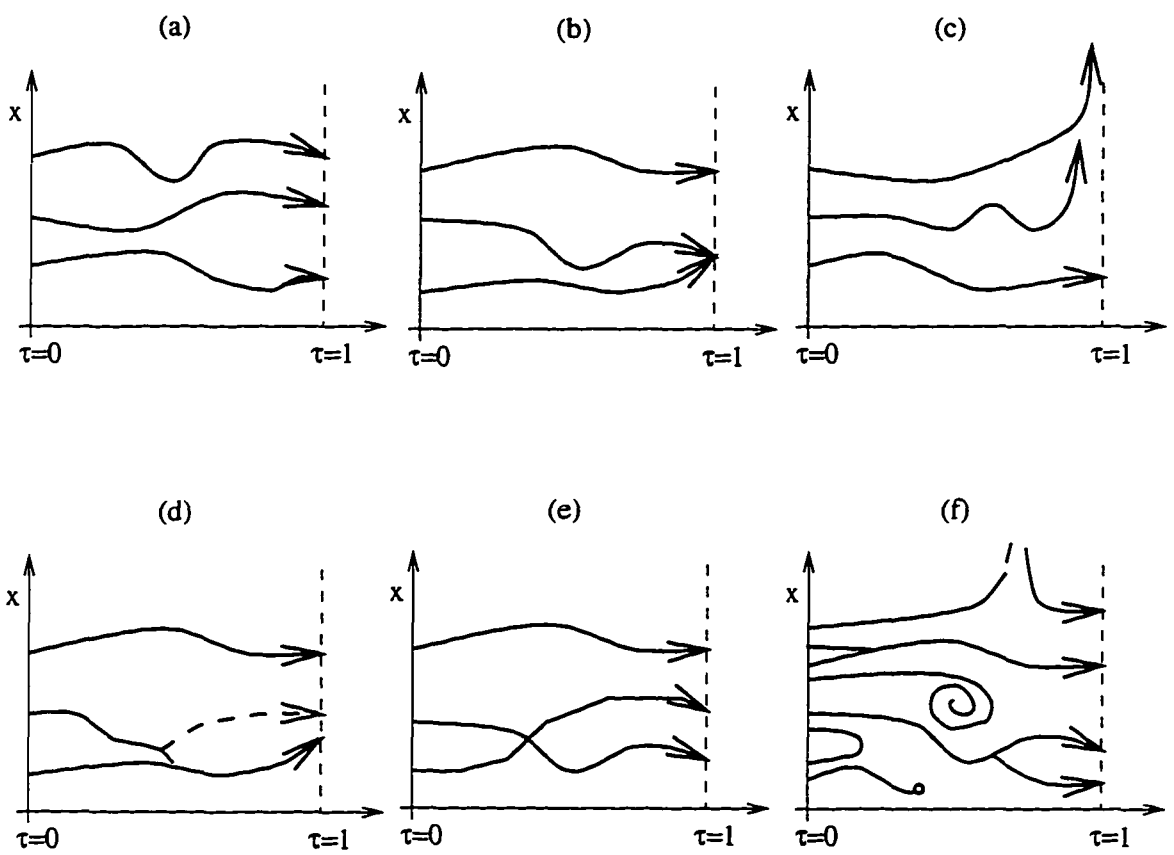

Figure 3.4 The path behavior of polynomial systems (a) non-overlapped, bounded paths (b) paths with multiplicity (c) diverging paths (d) path merged (e) path crossing (f) non-paths

Univariate Polynomial

Consider a polynomial of degree d represented by $f(x)$.

$$f(x) = a_d x^d + a_{d-1} x^{d-1} + ... + a_1 x + a_0 = 0, \tag{3.25}$$

The starting function is chosen to be

$$g(x) = p^d x^d - q^d = 0 \tag{3.26}$$

The solutions of $g(x) = 0$ are d equally spaced points on a circle of radius $|q|/|p|$ in the complex plane expressed as,

$$x = \frac{q}{p}\left(\cos\frac{2\pi j}{d} + i\sin\frac{2\pi j}{d}\right), \; j = 1, 2, ..., d \tag{3.27}$$

A fundamental theorem of algebra states that every polynomial in one complex variable with degree d has the same number of solutions.

Here, p and q are independently chosen complex constants and d is the maximum degree of equation $f(x)$. This means that we choose the p and q to avoid certain special algebraic relationships implied by the structure of $h(x, \tau)$ and the coefficients of $f(x)$. Further discussion related to the independence of p and q with respect to the coefficients is presented in Appendix.

Two polynomials in Two Variables

Consider a target system consisting of two polynomials,

$$f_1(x, y) = \sum_{i=0}^{c_x}\sum_{j=0}^{c_y} a_{ij} x^i y^j = 0 \tag{3.28a}$$

$$f_2(x, y) = \sum_{k=0}^{e_x}\sum_{l=0}^{e_y} b_{kl} x^k y^l = 0 \tag{3.28b}$$

In this case, the starting functions are chosen as

$$g_1(x, y) = p_1^{d_1} x^{d_1} - q_1^{d_1} = 0 \tag{3.29a}$$

$$g_2(x, y) = p_2^{d_2} y^{d_2} - q_2^{d_2} = 0 \tag{3.29b}$$

Notice that each starting function is a function of only one variable, either x or y. The degrees $d_1 = c_x + c_y$ and $d_2 = e_x + e_y$ are obtained from the maximum degree of $f_1(x, y)$ and $f_2(x, y)$, respectively. The coefficients p_1, q_1, p_2 and q_2 are chosen independent of the coefficients of $f_1(x, y)$ and $f_2(x, y)$, as described earlier.

The total number of paths, which are equivalent to the total number of solutions satisfying $f_1(x, y) = 0$ and $f_2(x, y) = 0$, simultaneously, is in this case, $d_1 \times d_2$. In contrast to the case of one polynomial systems, the paths can diverge in the multiple polynomial system. The number of diverging paths depends on the number of solutions at infinity. A solution at infinity of a polynomial system is defined as the solution of its homogeneous part. It is not possible to know how many paths will be diverging by looking at the homogeneous part of the target function since there can be multiple paths diverging for a single solution at infinity. The Bezout theorem [60] states the relation between the number of finite solutions and the number of solutions at infinity as follows:

1. Unless a system has an infinite number of solutions, the number of its solutions is less than or equal to its total degree.

2. Unless a system has an infinite number of finite solutions or an infinite number of solutions at infinity, the number of its finite solutions and its solutions at infinity add up to exactly the total degree, counting multiplicities.

4 APPLICATION OF HCM TO ADAPTIVE IIR FILTER DESIGN

This chapter describes the modification of the basic HCM discussed in Chapter 3. The modified HCM is used in constructing a new iterative algorithm for estimating the coefficients of adaptive IIR filters.

It will be first shown that the IIR filter design problem can be formulated in terms of a set of polynomial equations with time varying coefficients. The HCM is then modified to solve polynomial equations with time varying coefficients. The implementation of the new algorithm on a first-order filter example is demonstrated. Through this example, the parameters influencing the performance of the proposed algorithm are studied. Other aspects of the modified homotopy continuation, including convergence properties are also investigated. The method is then implemented on a second-order filter. Variations in filter structure are then evaluated for improving the performance of the basic structure of the filter.

Polynomial Representation of IIR Filter Design Problem

Adaptive IIR filtering operation can be described by a set of polynomials with time-varying coefficients, where the coefficients are estimated using instantaneous values of the cross-correlation of input and output signals of an unknown system.

Consider the system identification example shown in Figure 2.1. The filter is repre-

sented by the transfer function

$$W(z) = \frac{A(z)}{B(z)} = \frac{\alpha_0 + \alpha_1 z^{-1} + ... + \alpha_p z^{-p}}{1 - \beta_1 z^{-1} - ... - \beta_q z^{-q}} \equiv \frac{A(z)}{B(z)} \ , p < q \tag{4.1}$$

and the unknown system to be identified is represented by

$$V(z) = \frac{C(z)}{D(z)} \tag{4.2}$$

The following notations are used to represent signals.

- $d(n)$: desired signal or unknown system output
- $u(n)$: input signal to the unknown system the filter
- $y(n)$: filter output signal
- $e(n)$: error signal, $d(n) - y(n)$
- $V(z), v(n)$: unknown system
- $A(z), a(n)$: moving average (MA) part of the unknown system
- $B(z), b(n)$: auto-regressive (AR) part of the unknown system
- $W(z), w(n)$: filter, model
- $C(z), c(n)$: moving average (MA) part of the filter
- $D(z), d(n)$: auto-regressive (AR) part of the filter
- $\Phi(z), \phi(n)$: correlation function
- $\hat{\Phi}(z), \hat{\phi}(n)$: estimated correlation function

The expected value of the mean squared error (MSE) is given as

$$E[e^2(n)] = E[(d(n) - y(n))^2] \tag{4.3}$$

Performing the expectation operation and assuming stationarity of all signals results in the following expression for the MSE as a function of correlation terms [7]:

$$\begin{aligned}
\xi &= E[(d(n)-y(n))^2] && (4.4a)\\
&= E[d^2(n)-2d(n)y(n)+y^2(n)] && (4.4b)\\
&= E[d^2(n)]-2E[d(n)y(n)]+E[y^2(n)] && (4.4c)\\
&= \phi_{dd}(0)-2\phi_{yd}(0)+\phi_{yy}(0) && (4.4d)
\end{aligned}$$

where ϕ's represent correlation functions. The correlation ϕ_{dd}, ϕ_{yd} and ϕ_{yy} are expressed as a function of filter parameters as follows.

$$\begin{aligned}
\phi_{dd}(0) &= \phi_{dd}(n)|_{n=0}\\
&= Z^{-1}[|V(z)|^2\Phi_{uu}(z)]|_{n=0}\\
&= \frac{1}{2\pi j}\oint_{|z|=1}\frac{|C(z)|^2}{|D(z)|^2}\Phi_{uu}(z)z^{n-1}dz|_{n=0}\\
&= \frac{1}{2\pi j}\oint_{|z|=1}\frac{|C(z)|^2}{|D(z)|^2}\Phi_{uu}(z)\frac{dz}{z} && (4.5a)\\
\phi_{yy}(0) &= \phi_{yy}(n)|_{n=0}\\
&= Z^{-1}[|W(z)|^2\Phi_{uu}(z)]|_{n=0}\\
&= \frac{1}{2\pi j}\oint_{|z|=1}\frac{|A(z)|^2}{|B(z)|^2}\Phi_{uu}(z)z^{n-1}dz|_{n=0}\\
&= \frac{1}{2\pi j}\oint_{|z|=1}\frac{|A(z)|^2}{|B(z)|^2}\Phi_{uu}(z)\frac{dz}{z} && (4.5b)\\
\phi_{yd}(0) &= \phi_{dy}(0)\\
&= \phi_{dy}(n)|_{n=0}\\
&= Z^{-1}[\frac{W(z)}{V(z)}\Phi_{dd}(z)]|_{n=0}\\
&= Z^{-1}[\frac{W(z)}{V(z)}|V(z)|^2\Phi_{uu}(z)]|_{n=0}\\
&= Z^{-1}[W(z)V(z^{-1})\Phi_{uu}(z)]|_{n=0}\\
&= \frac{1}{2\pi j}\oint_{|z|=1}\frac{A(z)}{B(z)}\frac{C(z^{-1})}{D(z^{-1})}\Phi_{uu}(z)z^{n-1}dz|_{n=0}\\
&= \frac{1}{2\pi j}\oint_{|z|=1}\frac{A(z)}{B(z)}\frac{C(z^{-1})}{D(z^{-1})}\Phi_{uu}(z)\frac{dz}{z} && (4.5c)
\end{aligned}$$

We assume the autocorrelation function $\phi_{uu}(n)$ is an impulse function given by

$$\phi_{uu}(n) = \delta(n) = \begin{cases} 1 & ,n = 0 \\ 0 & ,\text{otherwise} \end{cases} \tag{4.6a}$$

$$\Phi_{uu}(z) = Z[\phi_{uu}(n)] = 1 \tag{4.6b}$$

and, from Eq. (4.4) through Eq. (4.5), the MSE ξ can be rewritten as

$$\begin{aligned} \xi &= \frac{1}{2\pi j}\oint_{|z|=1}\frac{|C(z)|^2}{|D(z)|^2}\frac{dz}{z} + \frac{1}{2\pi j}\oint_{|z|=1}\frac{|A(z)|^2}{|B(z)|^2}\frac{dz}{z} - \frac{2}{2\pi j}\oint_{|z|=1}\frac{A(z)}{B(z)}\frac{C(z^{-1})}{D(z^{-1})}\frac{dz}{z} \\ &= \frac{1}{2\pi j}\oint_{|z|=1}\frac{|C(z)|^2}{|D(z)|^2}\frac{dz}{z} + \frac{1}{2\pi j}\oint_{|z|=1}\frac{A(z)}{B(z)}\frac{A(z^{-1})}{B(z^{-1})}\frac{dz}{z} - \frac{2}{2\pi j}\oint_{|z|=1}\frac{A(z)}{B(z)}V(z^{-1})\frac{dz}{z} \end{aligned} \tag{4.7}$$

Note that the first term in the autocorrelation function $\phi_{dd}(n)$ of the desired signal $d(n)$ is not a function of filter coefficients. The filter is assumed to be stable, so that the poles of $\frac{A(z)}{B(z)}$ are located inside the unit circle and, hence, the poles of $\frac{A(z^{-1})}{B(z^{-1})}$ are outside the unit circle. The unknown system is also assumed to be stable, so that the poles of $V(z^{-1}) = \frac{C(z^{-1})}{D(z^{-1})}$ are located outside the unit circle. Therefore, the inverse z-transform for the second and third terms can be computed according to the residue theorem when $B(z)$ can be factorized.

The polynomials representing least mean squared error with respect to filter coefficients can be obtained from partial derivative of the error function with respect to filter coefficients as

$$\frac{\partial\xi}{\partial\alpha_i} = 0 = \frac{\partial}{\partial\alpha_i}\left[\frac{1}{2\pi j}\oint_{|z|=1}\frac{A(z)}{B(z)}\frac{A(z^{-1})}{B(z^{-1})}\frac{dz}{z}\right] - \frac{\partial}{\partial\alpha_i}\left[\frac{2}{2\pi j}\oint_{|z|=1}\frac{A(z)}{B(z)}V(z^{-1})\frac{dz}{z}\right] \quad ,i = 0,1,...,p \tag{4.8a}$$

$$\frac{\partial\xi}{\partial\beta_j} = 0 = \frac{\partial}{\partial\beta_j}\left[\frac{1}{2\pi j}\oint_{|z|=1}\frac{A(z)}{B(z)}\frac{A(z^{-1})}{B(z^{-1})}\frac{dz}{z}\right] - \frac{\partial}{\partial\beta_j}\left[\frac{2}{2\pi j}\oint_{|z|=1}\frac{A(z)}{B(z)}V(z^{-1})\frac{dz}{z}\right] \quad ,j = 1....,q \tag{4.8b}$$

The polynomials obtained in this manner depend on the choice of the order of filter model. These polynomial expressions are next derived for the cases of a first and a second order filters.

First-order IIR Filter

Consider a first-order filter represented as

$$W(z) = \frac{A(z)}{B(z)} = \frac{\alpha}{1 - \beta z^{-1}} \tag{4.9}$$

There is a single pole β in this case, with a simple inverse z-transform [9]. From Eq. (4.7),

$$\xi = \phi_{dd}(0) + \frac{\alpha^2}{1-\beta^2} - 2\alpha V(z) \mid_{z^{-1}=\beta} \tag{4.10a}$$

$$= \phi_{dd}(0) + \frac{\alpha^2}{1-\beta^2} - 2\alpha \sum_{i=0}^{L} v(i)\beta^i \tag{4.10b}$$

Differentiating above equation with respect to α and β results in the following polynomials.

$$\frac{\partial \xi}{\partial \alpha} = \alpha - (1-\beta^2)\sum_{i=0}^{L} v(i)\beta^i = 0 \tag{4.11a}$$

$$\frac{\partial \xi}{\partial \beta} = \alpha\beta - (1-\beta^2)^2 \sum_{i=0}^{L} iv(i)\beta^{i-1} = 0 \tag{4.11b}$$

The impulse response of the unknown system, $v(i) = Z^{-1}[V(z)]$, is infinitely long, i.e., $L = \infty$.

Since α is unique for β, Eq. (4.11a) and Eq. (4.11b) can be combined to a single polynomial in β as

$$(1-\beta^2)\left[\beta \sum_{i=0}^{L} v(i)\beta^i - (1-\beta^2)\sum_{i=0}^{L} iv(i)\beta^{i-1}\right] = 0 \tag{4.12}$$

The term $(1-\beta^2)$ can be omitted since the solution ± 1 do not represent stable solutions.

Second-order IIR Filter Case

When the unknown system is modeled by a second-order filter which is represented as

$$W(z) = \frac{\alpha}{1 - 2\beta_1 z^{-1} - \beta_2 z^{-2}} \tag{4.13}$$

the denominator can be factorized as

$$\begin{aligned} W(z) &= \frac{\alpha}{1 - 2\beta_1 z^{-1} - \beta_2 z^{-2}} && (4.14a) \\ &= \frac{\alpha z^2}{z^2 - 2\beta_1 z - \beta_2} && (4.14b) \\ &= \frac{\alpha z^2}{[z - (\beta_1 + \sqrt{\beta_1^2 + \beta_2})][z - (\beta_1 - \sqrt{\beta_1^2 + \beta_2})]} && (4.14c) \end{aligned}$$

Define the poles as

$$\begin{aligned} p_+ &= \beta_1 + \sqrt{\beta_1^2 + \beta_2} && (4.15a) \\ p_- &= \beta_1 - \sqrt{\beta_1^2 + \beta_2} && (4.15b) \end{aligned}$$

and

$$r(i) = \frac{p_+^i - p_-^i}{p_+ - p_-} \tag{4.16}$$

Then,

$$\begin{aligned} \phi_{yy}(0) &= \frac{1}{2\pi j} \oint_{|z|=1} \frac{A(z)}{B(z)} \frac{A(z^{-1})}{B(z^{-1})} \frac{dz}{z} \\ &= \frac{\alpha^2(1 - \beta_2)}{(1 + \beta_2)[(1 - \beta_2)^2 - 4\beta_1^2]} && (4.17a) \\ \phi_{yd}(0) &= \frac{1}{2\pi j} \oint_{|z|=1} \frac{A(z)}{B(z)} V(z^{-1}) \frac{dz}{z} \\ &= \alpha \sum_{i=0}^{L} v(i) r(i+1) && (4.17b) \end{aligned}$$

and the MSE is given as

$$\xi = \frac{1}{2\pi j} \oint_{|z|=1} \frac{|C(z)|^2}{|D(z)|^2} \frac{dz}{z} + \frac{\alpha^2(1 - \beta_2)}{(1 + \beta_2)[(1 - \beta_2)^2 - 4\beta_1^2]} - 2\alpha \sum_{i=0}^{L} v(i) r(i+1) \tag{4.18}$$

The target polynomials to be solved can be obtained as [62]

$$\frac{\partial \xi}{\partial \alpha} = \alpha(1-\beta_2) - (1+\beta_2)[(1-\beta_2)^2 - 4\beta_1^2]\sum_{i=0}^{L} v(i)r(i+1) = 0 \tag{4.19a}$$

$$\frac{\partial \xi}{\partial \beta_1} = 4\alpha\beta_1(1-\beta_2) - (1+\beta_2)[(1-\beta_2)^2 - 4\beta_1^2]^2\sum_{i=0}^{L} v(i)\frac{\partial r(i+1)}{\partial \beta_1} = 0 \tag{4.19b}$$

$$\frac{\partial \xi}{\partial \beta_2} = \alpha[\beta_2(1+\beta_2)^2 - 4\beta_1^2] - (1-\beta_2)^2[(1-\beta_2)^2 - 4\beta_1^2]^2\sum_{i=0}^{L} v(i)\frac{\partial r(i+1)}{\partial \beta_2} = 0 \tag{4.19c}$$

The three polynomials can be reduced two polynomials using the uniqueness of α.

Cross-correlation Function

The impulse response of the plant $v(i)$ is equivalent to the cross-correlation function $\phi_{ud}(i)$, when the autocorrelation function of the input signal is an impulse function with unit variance [63].

$$\phi_{ud}(i) = v(i) * \phi_{uu}(i) = v(i) * \delta(i) = v(i) \tag{4.20}$$

where $*$ represents a convolution. We can easily obtain the instantaneous estimate of $v(i)$ by taking average of $u(n)d(n-i)$ of a few input and desired output samples.

In order to get an accurate estimate of β, it is necessary to calculate $v(i)$ for all i, which is not practical. Instead, we approximate $v(i)$ to a finite length L. This does not mean that the filter is an FIR filter but, rather, we consider only the dominant part of the plant output by using a finite number of terms in the impulse response. The number of solutions to be tracked is determined by the value of L.

As an example, when $L = 5$, in the one-pole filter, the polynomial to be solved is, from Eq. (4.12),

$$\begin{aligned} 5v(5)\beta^5 + (4v(3) - 5v(5))\beta^4 + (3v(2) - 4v(4))\beta^3 + \\ (2v(1) - 3v(3))\beta^2 + (v(0) - 2v(2))\beta - v(1) \;=\; \\ 5\phi_{ud}(5)\beta^5 + (4\phi_{ud}(3) - 5\phi_{ud}(5))\beta^4 + (3\phi_{ud}(2) - 4\phi_{ud}(4))\beta^3 + \end{aligned} \tag{4.21a}$$

$$(2\phi_{ud}(1) - 3\phi_{ud}(3))\beta^2 + (\phi_{ud}(0) - 2\phi_{ud}(2))\beta - \phi_{ud}(1) = 0 \quad (4.21b)$$

The true coefficients of the polynomials are not available and, in adaptive filtering, the filter is supposed to adapt to slow changes in the unknown plant characteristics. The degree of the polynomial determined by L decides the number of solution paths, which in turn decides the processing complexity. Hence, there is a trade-off relation between the accuracy of filter coefficients and system complexity that governs the choice of L.

In adaptive filtering, the estimates of polynomial coefficients differ from the true values which can be obtained using an exact cross-correlation function of input and output signal of the unknown system or plant. The coefficients of the polynomial are estimated from a short-time observation of input and output signal of the plant, i.e.,

$$\hat{v}(i,n) = \hat{\phi}_{ud}(i,n) = \frac{1}{K-1} \sum_{k=n}^{n-K+1} u(k)d(k-i) \quad (4.22)$$

assuming that $\hat{\phi}_{ud}(i,n)$ approaches the true cross-correlation $\phi_{ud}(i)$ function when K, the number of samples, increases to infinity and the unknown system is stationary.

Modification of The Homotopy Continuation Method

In this section, the homotopy continuation method is modified for solving polynomial equations with time varying coefficients. Hence, the Lth-degree polynomial equation is a function of time n as well as x.

$$f(x,n) = a_L(n)x^L + a_{L-1}(n)x^{L-1} + ... + a_1(n)x + a_0(n) \quad (4.23a)$$

$$= [a_L(n)\ a_{L-1}(n)\ ...\ a_o(n)][x^L\ x^{L-1}\ ...\ 1]^T \quad (4.23b)$$

Assuming the coefficients are characterized by statistical properties, i.e., means and variances, we can consider an equation with coefficients obtained from the mean values as

$$f(x) = E[f(x,n)] \quad (4.24a)$$

$$= E[a_L(n)]x^L + E[a_{L-1}(n)]x^{L-1} + ... + E[a_0(n)] = 0 \qquad (4.24b)$$

In a situation when the true means are not available, and only average values in short intervals or instantaneous estimates, are observable, the HCM is modified to solve $E[f(x,n)]$ by tracking the solution paths of $f(x,n)$ as $n \to \infty$. In this case, we have

$$h(x,\tau,n) = (1-\tau)g(x) + \tau f(x,n) = 0 \qquad (4.25)$$

i.e., the homotopy function is now a function of time n as well as τ and x. The function $g(x)$ is not affected by time n. One basic assumption is that the solutions and solution paths do not vary too much from the mean. If the solution paths of the function with time varying the coefficients vary widely and rapidly, path mergings occur, and the algorithm fails to reach the desired solution or converges very slowly.

The modified homotopy continuation method, namely adaptive HCM (AHCM), uses the following prediction-correction iteration algorithm illustrated in Figure 4.1.

1. *Prediction:* *At iteration step n, we have a solution $(x_j(n), \tau(n))$ to $h(x,\tau,n) = 0$ where $f(x,n)$ has coefficients vector $[a_L(n)\ a_{L-1}(n)\ ...\ a_1(n)\ a_0(n)]^T$, for the jth solution path. The next position $(x_j^*(n+1), \tau(n+1) = \tau(n) + \Delta\tau)$ is predicted from the current position $(x_j(n), \tau(n))$ in the direction of increasing τ.*

2. *Estimate coefficients:* *At the next step $n \to n+1$, a new coefficient vector of $f(x,n+1)$ $[a_L(n+1)\ a_{L-1}(n+1)\ ...\ a_1(n+1)\ a_0(n+1)]^T$. is estimated.*

3. *Correction:* *the current position $(x_j^*(n+1), \tau(n+1))$ is corrected to the closest $(x_j(n+1), \tau(n+1))$ to satisfy $h(x,\tau,n+1) = 0$ using Newton method.*

Notice that the correction is performed using the new coefficient vector estimated at the $(n+1)$ step, hence the correction step provides the way to jump to the incoming function. The steps (1) through (3) are iterated until τ reaches 1. When τ exceeds 1. the increment $\Delta\tau$ turns into a negative value so that τ stays around 1. It is seen that

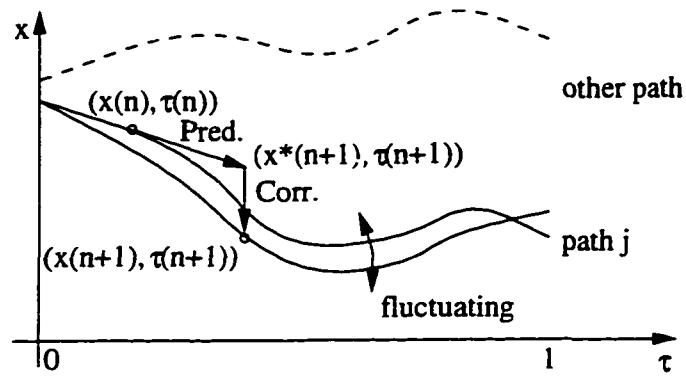

Figure 4.1 The prediction and correction step for path tracking in AHCM

the algorithm is able to track solutions of the polynomial even when the signals are not stationary, for example, when the mean of the polynomial coefficients vary slowly in time. Thus, the algorithm has the capability of true adaptation.

At the end of the iteration, the solution path reaches the instantaneous solution of the function. The desired average solution is obtained as

$$a_j = (1-\mu)a_j(n) + \mu a_j(n+1), \quad j = 1, 2, ..., L \tag{4.26}$$

where μ is a convergence parameter. Now, the solution to the instantaneous homotopy function will converge to the desired average solution by constraining μ to be less than 1. It is shown later that the convergence rate of overall algorithm depends on μ and step size $\Delta\tau$.

Path Merging

One of the problems encountered in the correction step is path merging. During the correction step, using the Newton method, on the incoming homotopy function $h(x, \tau, n+1) = 0$, at a particular $\tau = \tau(k+1)$ two different predicted positions, $x_j^*(n)$ and $x_{j+1}^*(n)$ corresponding to jth and $(j+1)$th path could possibly be corrected to the same $x(n+1)$. Some strategies to prevent path merging are suggested below:

- A simple method to avoid path merging is to remove the root $x = x_j^*(n)$ from the homotopy function $h(x, \tau, n+1)$ by means of factorization before correction for the $(j+1)$th trajectory is performed, as follows,

$$\hat{h}(x, \tau, n+1) = \frac{h(x, \tau, n+1)}{x - x_j^*(n)} \tag{4.27}$$

- The factorization suggested above requires a significant amount of computation when polynomials are of a high degree. Path merging occurs, basically, when corrections are directed to the same position. Consequently, an alternate, simpler method is to skip the current iteration step, discard the estimated coefficients of polynomials and return to the previous step by recovering previous correction positions.

- Path merging can also occur when predictions at two neighboring paths are too close. Another method to prevent path merging is to "scale" the maximum predictions by a specified factor, so the separation distance between neighboring paths is maintained at a desired value enough to avoid path merging.

- Path merging can also be achieved by using a hybrid method combining both, the second and third method.

Even though the first technique requires more computation than the others, it offers superior speed of convergence in terms of the number of iteration steps. Whereas, the other methods are based on simple decision processing, the number of iteration steps for convergence is increased.

Simplification of Correction Step

As described in Chapter 3, the Newton method is most widely used in the correction step. The computational complexity involved in the matrix inversion in Newton method

or its simplified versions are known to be $O(N^3)$ or $O(N^2)$, respectively, where N is the dimension of data. To reduce the computational complexity, Morgan [55] suggested a simplified correction step in which the Jacobian matrix and its inverse are calculated only once and reused for succeeding iterations.

In this method, the correction step for finding the true solution using the Newton method is modified from Eq. (3.38) to the form

$$\vec{x}^{k+1} = \vec{x}^{k} - \frac{H(\vec{x}^{k}, \tau^{i})}{H'_{\vec{x}}(\vec{x}^{0}, \tau^{i})} \tag{4.28}$$

where $\vec{x}^{0}$ is the predicted value at ith prediction-correction step and the starting position of the correction step. $H'_{\vec{x}}(\vec{x}^{0}, \tau^{i})$ and its inverse are calculated at the first iteration and reused.

However, this procedure results in slower convergence speed since the slope of the homotopy function estimated near the predicted position is usually more steep than that of true solution which is usually closer to the stationary point of the convex function [64]. However, by using the same slope continuously, the computational complexity of the succeeding iteration is reduced to $O(N)$ since the Jacobian, $H'_{\vec{x}}(\vec{x}^{0}, \tau^{i})$ and its inverse are calculated once at the beginning of the correction.

The overall order of computational complexity of path tracking using prediction and correction by HDE or BDE still remains at $O(N^3)$ since each prediction and correction step requires an inversion operation of the Jacobian matrix. There have been many efforts to reduce the computational burden occurring in matrix inversion, especially, in adaptive filtering applications[65] [66]. However, in this study, it is shown that, in a modified structure of the proposed algorithm, the high burden of matrix inversion can be avoided by reducing the order of filters to one or two, where the matrix inversion is not required or can be done in $O(N)$.

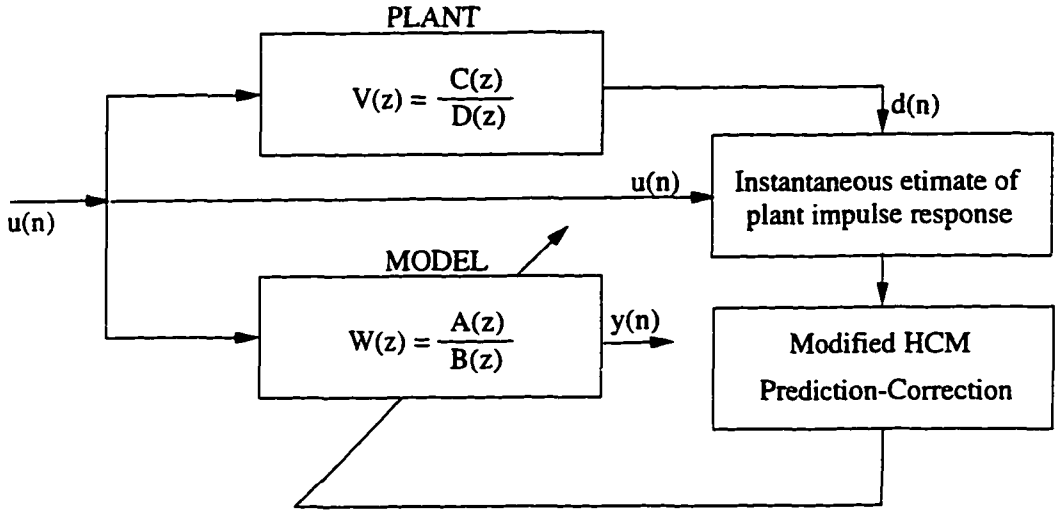

Figure 4.2 The structure of an AHCM IIR filter

AHCM Algorithm for IIR Filtering

In the filtering algorithm proposed here, the filtering operation consists of two steps: estimation of cross-correlation function, for determining the coefficients of polynomials, and solution path tracking using prediction and correction steps. The schematic of the adaptive IIR filter using the AHCM algorithm is shown in Figure 4.2. The parameter updating algorithm does not use the error between filter output signal and plant output signal directly unlike most adaptive IIR filtering algorithms do.

The procedure for AHCM IIR filtering is as follows:

1. *Determine the order of filter, p and q.*

2. *Obtain the governing polynomial equations after selecting an appropriate value of order of polynomials L.*

3. *Construct a homotopy function $h(x, \tau)$,*

4. *Select an appropriate value of number of samples K for estimating the cross-correlation function $\phi_{ud}(i, n)$, and determine values of stepsize $\Delta\tau$ and convergence*

parameter μ.

5. *Run the prediction-correction iteration for finding filter coefficients.*

   (a) Estimate $\phi_{ud}(i,n)$, i.e., the coefficients of polynomials, using the filter input $u(n)$ and output $y(n)$.

   (b) Predict the next solution of the paths corresponding to incremented homotopy parameter $\tau+\Delta\tau$ using either an HDE-based or BDE-based prediction method explained in Chapter 2.

   (c) Estimate the next set of coefficients of polynomials by observing the input and output of the unknown system.

   (d) Correct the solutions to the closest position using Newton method as shown.

The steps (1) through (4) are off-line procedures to construct the polynomial equations for IIR filtering problem before the iterative processing starts. The step (5) is repeated until the desired solutions are found.

AHCM Parameters

As mentioned before, the complexity and performance of the algorithm depend on several parameters. In the construction of polynomials representing the filtering operation, we need to choose L, the order of polynomials, and K, the number of samples to be used in the estimation of the cross-correlation function. The complexity of the algorithm and accuracy of the solution are determined by the selection of both parameters, L and K.

Two other parameters that influence the numerical performance of the AHCM are step size $\Delta\tau$ and convergence parameter μ. The two parameters represent a trade off between the convergence rate and accuracy of the algorithm.

- order of polynomial L: complexity vs. accuracy

  Optimum values of coefficients of an IIR filter can be obtained by AHCM only when L is infinite. However, a finite value has to be chosen in practice and hence the maximum degree of homotopy polynomials is determined by L. The computational complexity of filtering operation increases with the order L of the polynomials. A lower value of L results in a poorer accuracy of the global minimum position estimated.

- number of samples K': complexity vs. possibility of path merging.

  The K' and μ parameters determine the degree of adaptivity of a filter to changes in the unknown system. A large K' (and, a small μ) prevents a quick response to a change in the dynamics of the unknown system. A small K' (a large μ) causes the estimate $\phi_{ud}(n)$ to deviate too far from its mean value, resulting in path merging. Although both K' and μ affect the smoothness of the solution path, the unique role of K' comes from the fact that it is the only parameter affecting the actual coefficients of the polynomials. The large deviation of polynomial coefficients from a virtual mean can cause the correction to converge to a neighboring path or even to a path far away from the original path. Therefore, to avoid path merging, we want to keep the solution paths fluctuating near virtual average path by choosing a large K'. The number K' also affects the system complexity, especially, the storage requirement. When the value of K' is too small, the coefficients of polynomials change too rapidly, so the possibility of path merging increases. Whereas, when K' is too large, the adaptivity of the filter decreases since the filter can not respond quickly to changes in the unknown system.

- convergence parameter μ: convergence rate vs. possibility of path merging.

  The role of μ is basically identical to that of K'. However, μ controls the smooth-

ness of solution paths more directly than K'. The movement of solutions can be smoothed by choosing a small μ even when the polynomials vary rapidly due to the coarse estimation of $\phi_{ud}(n)$ caused by a small K. We can say, that K' and μ are mutually complementary in smoothing the solution paths. Both parameters K' and μ also determine the degree of adaptivity of a filter to changes in the unknown system. In other words, they influence the convergence speed to the optimum filter coefficients when the AHCM is working in a tracking mode.

- stepsize $\Delta\tau$: convergence rate vs. possibility of path merging.

  The effect of $\Delta\tau$ on the performance of the filter is similar to that of K' and μ. The value of $\Delta\tau$ affects the smoothness of paths in the prediction step. The predicted solutions are proportional to $\Delta\tau$. An excessive prediction due to a large $\Delta\tau$ may cause the solution to jump to other nearby paths, resulting in path merging. The parameter uniquely decides how fast the filter can change the operation mode from optimization (stationary signal processing) to tracking (non-stationary signal processing).

In summary, the accuracy of filter coefficients is largely dependent on the selection of L. The adaptivity of the filter is affected by the selection of K' and μ, and $\Delta\tau$ controls the convergence rate of the filter. The path smoothness is aslo a function of K', μ and $\Delta\tau$.

In the simulation examples in Chapter 5, the performance of the proposed algorithm with respect to the four parameters are presented.

Tracking Capability of AHCM Filters

A significant feature of adaptive filtering is its adaptability to changes in the unknown system. In the construction of AHCM filtering algorithm, we assume the characteristic

of the unknown system (i.e., transfer function) does not change rapidly during the period when the homotopy parameter τ increases from 0 to 1.

The convergence parameter μ and K enable the filter to track a slow change in the system characteristic. A sudden change in the system may cause the solution paths to deviate too far from its virtual mean, which results in path merging. In this case, the AHCM filter can be reset to follow a new system by initializing $\tau = 0$.

When the change in the unknown system occurs after the τ reached 1, the capability of an AHCM filter to track the change largely depends on the magnitude of the change. If the new global minimum position is too far from present position, the solution path which found the present global minimum fails to converge to the new one. Other solution paths which found local minima may converge to the new global minimum position. In the worst case, when the tracking fails, the AHCM filter can be reset by initializing τ to 0. The estimated MSE can be chosen as the criteria for determining whether the AHCM filter must be reset or not.

Advantages and Disadvantages of AHCM IIR Filters

The AHCM IIR filtering technique can theoretically determine the global minimum of the MSE surface. Also, the convergence speed is expected to be much faster than LMS-based adaptive filtering algorithms. Another major advantage of AHCM filtering is the property of stability. Since all possible solutions are tracked during AHCM, alternate values for filter coefficients are always available when filter pole escapes outside the unit circle. Alternate candidates for filter coefficients can be chosen from one of the remaining solutions according to minimum mean squre error criteria.

A noticeable drawback of AHCM IIR filtering is the selection of the polynomial order, L. The polynomial representation of practical ARMA filters requires choice of a finite number L. However, by selecting a finite value L, the minimization processing

by the AHCM IIR filter results in a degradation of filter performance. In other words, information in the tail of the impulse response of the unknown system does not contribute to the filter performance.

One possible way to solve this problem is to combine the conventional LMS approach with AHCM algorithm in such a way that, after the adaptive filter reaches a global minimum state by the AHCM algorithm, the LMS algorithm is employed for further minimization, so that information in the tail of system impulse response is completely considered by the LMS procedure. The initial starting values for the LMS filtering are provided by the AHCM, so that the convergence to a global minimum state is guaranteed with higher probability.

A more serious problem comes from the number of solution paths to be tracked, for higher order filters ($q \geq 2$). The number of paths increases geometrically with filter order. For example, the number of paths to be tracked for a two-pole filter is 24 when $L = 4$, as will be seen later in Chapter 5. As the number of solution paths increases, the algorithm is more susceptible to path merging, and more time is spent on avoiding path merging, resulting in poorer performance. A solution to this drawback is the multi-stage AHCM filtering, described later in this chapter.

AHCM-LMS Filter

As discussed in the last section, the selection of finite value of L results in an undesired degradation. As a simple solution, the conventional LMS algorithm can be employed to complete the convergence of the filter coefficients to the global minimum. With a sufficiently large L, the global minimum reached by AHCM filtering is always located close to an ideal global minimum corresponding to an infinite L. By initializing the starting values of the LMS filter with the global minimum coefficients obtained by the AHCM filter, the probability of convergence to the ideal global minimum with the LMS

filter can be maximized. However, the convergence to the ideal global minimum using the LMS filter is not always guaranteed, since the LMS filter, based on a stochastic movement, may converge to the nearest local minimum.

When a filter output signal is represented as

$$y(n) = \sum_{i=1}^{q} \beta_i(n) y(n-i) + \sum_{j=0}^{p} \alpha_j(n) u(n-j), \tag{4.29}$$

the conventional LMS-based IIR filtering [5] is summarized as

$$\delta\vec{\theta}(n) = \mu\vec{\phi}(n)e(n) \tag{4.30}$$

where

$$\vec{\phi}(n) = [y(n-1)\, y(n-2) \ldots y(n-q)\, u(n)\, u(n-1),,, u(n-p)]^T \tag{4.31a}$$

$$\vec{\theta}(n) = [\beta_1(n) \ldots \beta_q(n)\, \alpha_0(n) \ldots \alpha_p(n)]^T \tag{4.31b}$$

and

$$e(n) = d(n) - y(n) \tag{4.32a}$$

$$y(n) = \vec{\phi}(n)^T \vec{\theta}(n). \tag{4.32b}$$

and n denotes an iteration number.

In the combined filter, namely the AHCM-LMS filter, the LMS operation starts after the AHCM filter reaches the final state $\tau = 1$, as illustrated in Figure 4.3. When a tracking mode operation is required, the AHCM filter operates independently of the LMS part.

Multi-stage AHCM Filter

As shown in the case of a two-pole filter, the number of trajectories increase geometrically with the number of poles of the filter resulting in path merging. An alternative

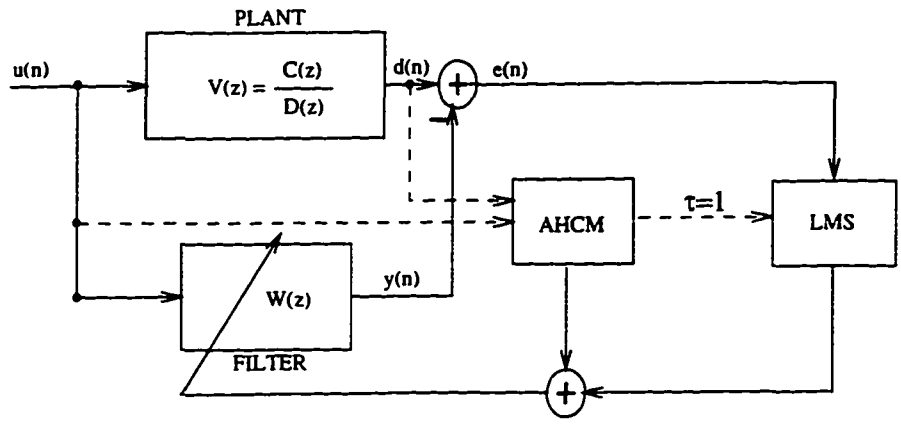

Figure 4.3 The structure of an AHCM-LMS filter

structure for handling the problem related to higher order filters is described in this section.

The proposed structure of the new filter, namely a multi-stage AHCM (MAHCM) filter, is illustrated in Figure 4.4. An MAHCM filter consists of multiple small order AHCM (or AHCM-LMS) filters cascaded serially. The filtering is performed sequentially rather than simultaneously. The AHCM1 filter, at the first stage, filters the $u(n)$ and generates an error signal, $e_1(n) = d_1(n) - y_1(n)$. The second stage filter AHCM2 filters the error signal, $e_1(n)$ with respect to the same input signal $u(n)$, generating $y_2(n)$, and so on. When N small-order AHCM filters are cascaded in this manner, the total transfer function is derived as follows.

$$
\begin{aligned}
e_N(n) &= d_N(n) - y_N(n) && \text{(4.33a)}\\
&= d_{N-1}(n) - y_{N-1}(n) - y_N(n) && \text{(4.33b)}\\
&= \ldots\\
&= d(n) - (y_1(n) + y_2(n) + \ldots + y_N(n)) && \text{(4.33c)}\\
&= d(n) - (w_1(n) * u(n) + w_2(n) * u(n) + \ldots + w_N(n) * u(n)) && \text{(4.33d)}\\
&= d(n) - y(n). && \text{(4.33e)}
\end{aligned}
$$

so, the total transfer function of an N-stage MAHCM filter is

$$W(z) = \frac{Y(z)}{U(z)} \tag{4.34a}$$

$$= W_1(z) + W_2(z) + ... + W_N(z) \tag{4.34b}$$

Consequently, the overall order of the N-stage MAHCM filter is equal to the sum of the orders of the AHCM filters at each stage. Notice that, in this structure, the multi-stage filter works sequentially with respect to the input signal $u(n)$, implying a cascade structure, but the expression of the transfer function $W(z)$ is such that it constitutes an Nth-order parallel form.

The number of roots to be tracked, in an N-stage MAHCM filter is $N \times L$. In the case of cascaded one-pole AHCM filters, the number of paths is much smaller than that of a higher-order single stage AHCM filter. Therefore, the suggested structure of the MAHCM filter enables us to build a more efficient high-order adaptive filter, that avoids path merging and converges to a global minimum. When we choose a two-pole AHCM filter for each stage, the overall performance of each stage might improve, so that the overall filter will require a reduced number of stages N than in the case of the first-order filters.

From the standpoint of processing speed, a MAHCM filter offers considerable savings than a higher-order AHCM filter since the number of paths to be tracked is greatly reduced.

The advantages of a low-order MAHCM (or MAHCM-LMS) filter over a high-order AHCM (or AHCM-LMS) filter structure are summarized as follows:

1. The number of paths to be tracked is greatly reduced. The structure is simply obtained as a cascade of a number of stages (N) of the individual AHCM filter of order L. The number of paths is given by $N \times L$.

2. When a one-pole AHCM filter is employed, for each stage of an MAHCM fil-

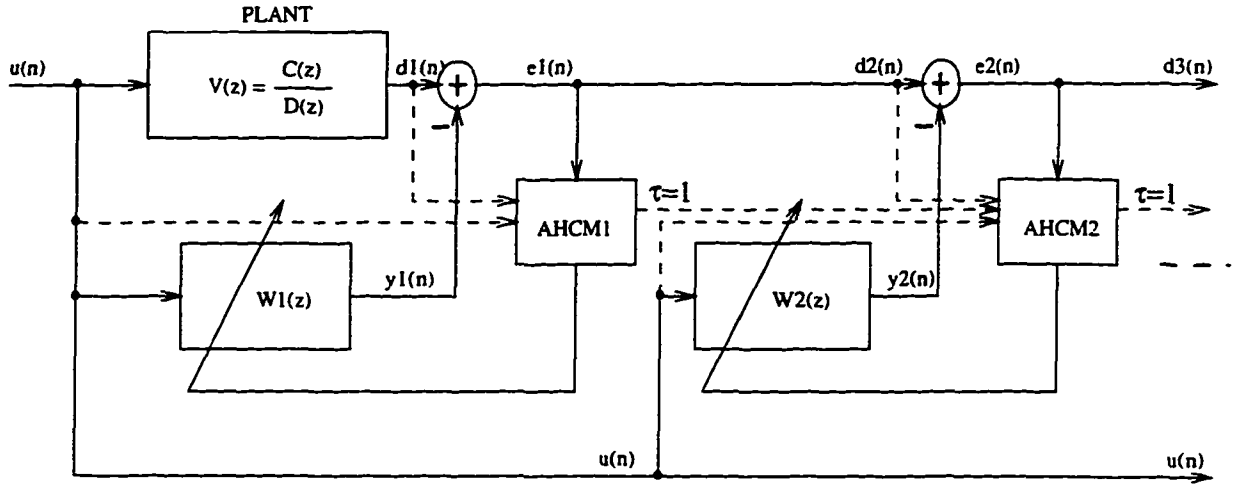

Figure 4.4 The structure of the MAHCM filter

ter, a solution path can diverge only if all coefficients of the polynomial are all zero. Therefore, the diverging paths can be detected easily in the MAHCM filter, whereas in a high-order (≥ 2) AHCM, the diverging paths are not immediately detectable.

3. Since the number of paths in the AHCM filter in each stage of an MAHCM filter is smaller, i.e., the path density is low and, the possibility of path merging is lower than that of a high order AHCM filter. This in turn results in faster convergence.

4. A most important advantage of the MAHCM filter is its capability to monitor the stability. Since the order of AHCM filters at each state is chosen to be small. the instability can be easily monitored by a factorization with less computation. Besides, when the order is chosen to be one, the factorization is not even necessary.

One disadvantage of the MAHCM filters is that the small-order AHCM filter at each stage models the desired signal $d_n(n)$, or the error signal $e_{n-1}(n)$ of the previous stage using an insufficient order modeling case.

5 SIMULATIONS AND DISCUSSIONS

In this chapter, the AHCM IIR filtering algorithm and its variations are simulated to solve system identification problem.

In the first section, two unknown systems with second- and third-order ARMA model are chosen for the simulation of a non-adaptive HCM modeling using a first-order and a second-order IIR filter. These unknown systems are reused in the second section for simulations of the adaptive HCM (AHCM) IIR filtering technique using the same first- and second-order IIR filters. The simulation results of the non-adaptive HCM modeling and AHCM IIR filtering are compared.

The performance of the AHCM filter in tracking capability is demonstrated, next, using the same unknown system. The effects of the AHCM parameters, K, μ, and $\Delta\tau$ on performance of the filter are evaluated by comparing convergence rate and path smoothness.

The AHCM-LMS and MAHCM filtering techniques suggested in Chapter 4 are also simulated for the same second-order unknown system, and the results are compared with those of the AHCM filter.

Non-Adaptive HCM Modeling

In Chapter 4, polynomials representing LMS operations with respect to filter coefficients were obtained. In this section, the HCM is applied directly to solve the polynomial systems of a first-order and a second-order filters. The coefficients of the polynomials are

obtained by observing the input and output of the unknown systems for a sufficiently long time, so that the signals are not time-varying. The roots obtained by this procedure will be used as the target filter coefficients values of the adaptive HCM (AHCM) filtering in which only a short-time observation of the input and output signals of the unknown system is allowed.

First-order IIR Filter

First, a one-pole filter is used to model an unknown plant characterized by a two-pole transfer function. This example has typically been used to evaluate and compare experimental adaptive filtering algorithms [7] [9].

The transfer function of the second order unknown system with auto-regressive and moving average (ARMA) structure is given as

$$V(z) = \frac{C(z)}{D(z)} = \frac{0.05 - 0.4z^{-1}}{1 - 1.1314z^{-1} + 0.25z^{-2}} \tag{5.1}$$

and the first-order IIR filter model is used to minimize the MSE. This is an example of under-modeling since the order of filter model is smaller than the order of unknown system.

The MSE surface in this case, shown in Figure 5.1, has one local minimum and one global minimum. The MSE is calculated by Eq. (4.6) when the autocorrelation function of the input signal is given as an impulse $\delta(\hat{u})$. The normalized MSE is computed by normalizing the MSE with the variance of the output signal.

The input signal used in the simulations, $u(n)$, is a normally distributed random signal with zero mean and unit variance. The autocorrelation function of the input signal is an impulse function, and the cross-correlation function $\phi_{ud}(n)$ is equivalent to the plant impulse response $v(n)$.

When the signal is stationary and time-invariant, very accurate values of the cross-correlation function of the plant, i.e., the coefficients of the polynomials, can be obtained

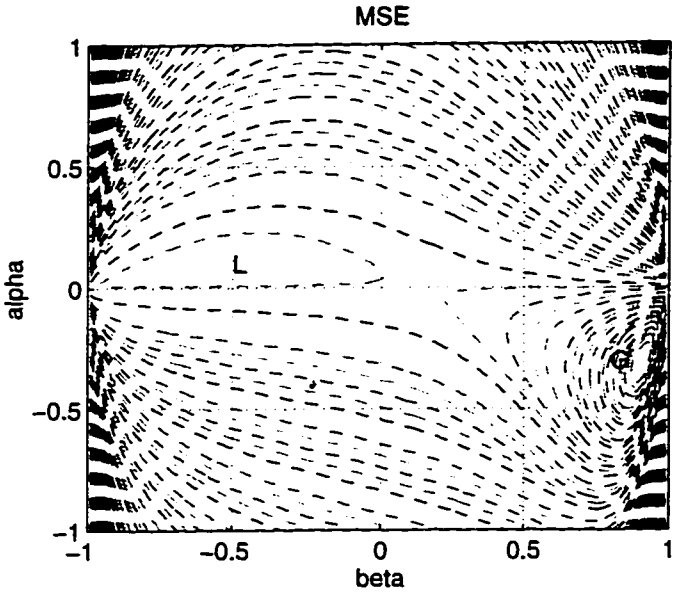

Figure 5.1 MSE surface of one-pole filtering

by observing the input and output signal for a sufficiently long time, (number of samples $K = \infty$). The polynomial to obtain optimum filter coefficient β, when the order of the polynomial $L = 5$, is given, from Eq. (4.21), as

$$f(x) = -1.5799x^5 - 1.4716x^4 + 0.0607x^3 + 0.4168x^2 + 0.8521x + 0.3434 \qquad (5.2)$$

where the unknown variable x represents the filter AR coefficient β. The solutions of $f(x)$ are $(0.839, -1.022, -0.144 + 728i, -0.144 - 0.728i, -0.461)$.

Since the order of polynomial is limited to $L = 5$, the solutions do not reach $\beta = 0.906$, but converge to $\beta = 0.839$. The MA filter coefficient $\alpha = -0.265$ is obtained either from Eq. (4.11a) or Eq. (4.11b). We can get a more accurate global minimum position by increasing the value of L, the approximation length of the plant impulse response. The filter coefficients, α and β, and MSE's found by the HCM modeling are listed in Table 5.1. Due to the finite value of L, the MSE obtained by an HCM modeling is not identical to the ideal one obtained using an LMS based filter. A practical solution

Table 5.1 MSE at global min. and local min., α and β by HCM modeling

Position	α	β	MSE	Norm.MSE
LMS, global	-0.311	0.906	0.207	0.277
LMS, local	0.144	-0.519	0.729	0.978
HCM, global	-0.285	0.839	0.301	0.404
HCM, local	0.118	-0.461	0.728	0.977

to achieve the ideal MSE with a finite L is described later in this chapter.

Figure 5.2 shows the solution paths starting from the five initial complex valued solutions which are equally spaced on a circle with radius 1.5, and ending at the solutions of $f(x) = 0$. One of the paths converges to the desired solution $\beta = 0.839$, which lies within the unit circle, and is stable.

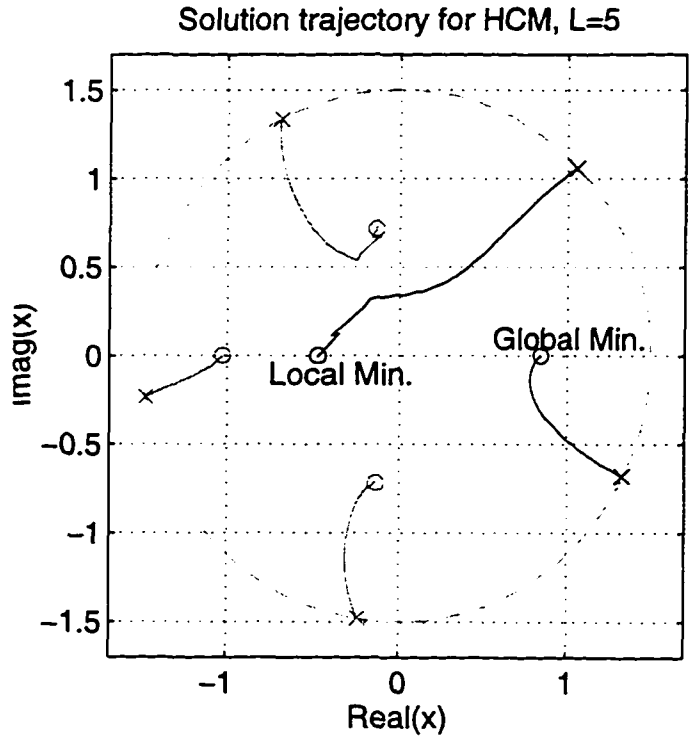

Figure 5.2 Solution paths of $f(\beta)$ with $\Delta\tau = 0.01$

The filter output with $(\alpha, \beta) = (-0.285, 0.839)$ and desired signal are compared in Figure 5.3. It is shown that the filter output signal follows the plant output signal faithfully.

Second-order IIR Filter

A similar system identification problem based on non-adaptive HCM modeling is next considered using a second order IIR filter. The unknown plant, having 3 poles and 2 zeros, is chosen to have the following transfer function.

$$V(z) = \frac{C(z)}{D(z)} = \frac{0.05 + 0.25z^{-1}}{1 - 0.4z^{-1} - 0.27z^{-2} + 0.09z^{-3}} \tag{5.3}$$

The transfer function of the filter, $W(z)$, with two poles is represented as

$$W(z) = \frac{A(z)}{B(z)} = \frac{\alpha_o}{1 - 2\beta_1 z^{-1} - \beta_2 z^{-2}} \tag{5.4}$$

The number of filter coefficients to be estimated is three, $\alpha_0, \beta_1, \beta_2$, and, from Eq. (4.19), the homotopy equation $\vec{h}(\vec{\beta}, \tau)$, $\vec{\beta} = [\beta_1\ \beta_2]^T$, are reduced to two equations. When $L = 4$,

$$\begin{aligned}
h_1(x = \beta_1, y = \beta_2, \tau) &= (1 - \tau)\, g_1(x, y, \tau) + \tau \\
&\{\ 128\phi_{ud}(3)x^4 - 24\phi_{ud}(3)x^2y^2 + 48\phi_{ud}(2)x^3 - 4\phi_{ud}(3)y^3 \\
&+\ 80\phi_{ud}(3)x^2y - 8\phi_{ud}(2)xy^2 + (16\phi_{ud}(1) - 24\phi_{ud}(3))x^2 \\
&+\ (8\phi_{ud}(3) - 2\phi_{ud}(1))y^2 + 20\phi_{ud}(2)xy + (4\phi_{ud}(0) - 8\phi_{ud}(2))x \\
&+\ (2\phi_{ud}(1) - 4\phi_{ud}(3))y - 2\phi_{ud}(1)\ \} \qquad (5.5a) \\
h_2(x = \beta_1, y = \beta_2, \tau) &= (1 - \tau)\, g_2(x, y, \tau) + \tau \\
&\{\ 8\phi_{ud}(3)x^3y^3 - 32\phi_{ud}(3)x^5 - 16\phi_{ud}(3)x^3y^2 \\
&+\ (4\phi_{ud}(2) - 16\phi_{ud}(3))x^2y^3 + 4\phi_{ud}(3)xy^4 + 4\phi_{ud}(3)y^5 \\
&-\ 16\phi_{ud}(2)x^4 - 8\phi_{ud}(3)x^3y - 12\phi_{ud}(2)x^2y^2 \\
&+\ (2\phi_{ud}(1) - 8\phi_{ud}(3))xy^3 + (2\phi_{ud}(2) - 8\phi_{ud}(3))y^4 - 8\phi_{ud}(1)x^3
\end{aligned}$$

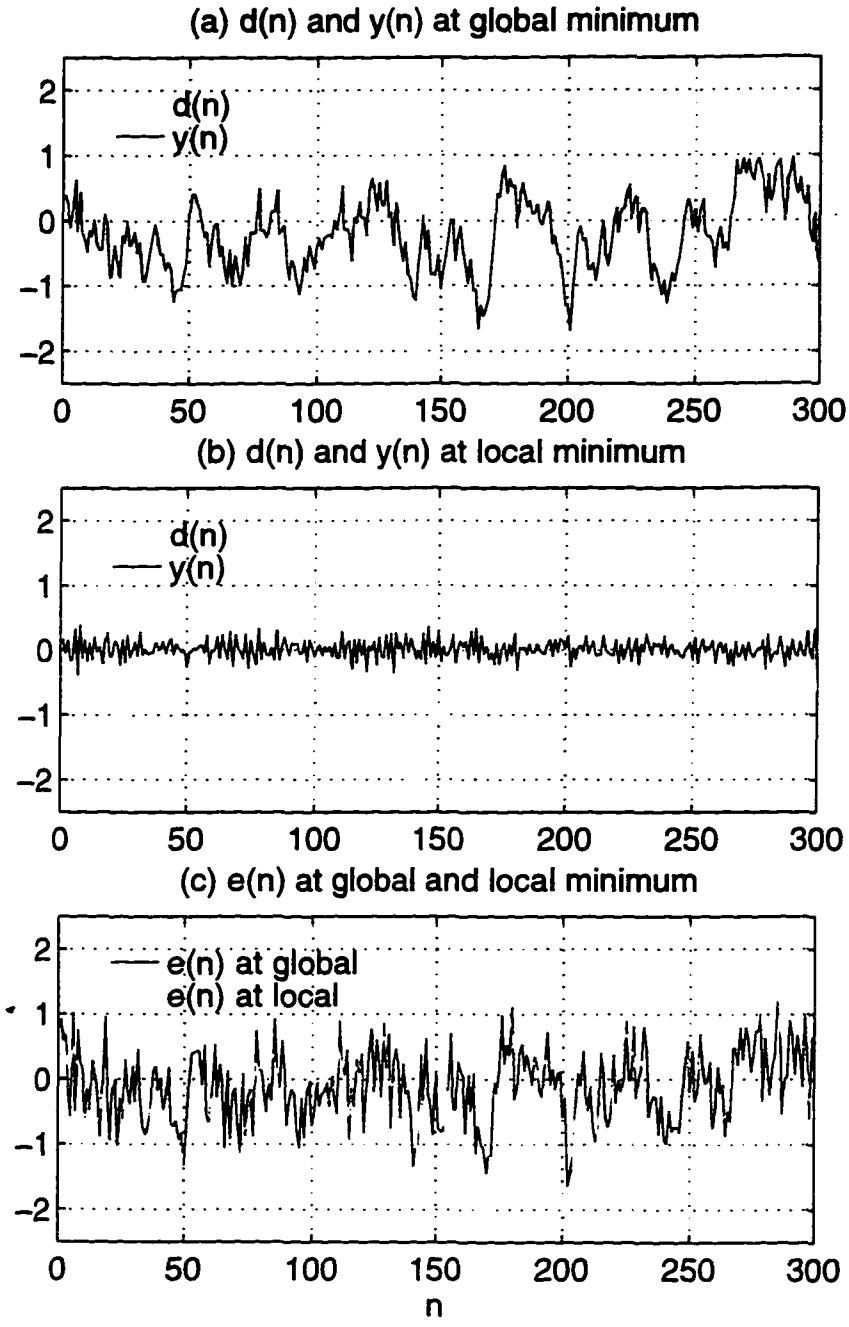

Figure 5.3 Filter output $y(n)$ and plant output $d(n)$ at (a) global minimum and (b) at local minimum, and (c) error $e(n) = d(n) - y(n)$

$$+ \; 16\phi_{ud}(3)x^2y + (4\phi_{ud}(3) - 4\phi_{ud}(1))xy^2 + (\phi_{ud}(0) - 4\phi_{ud}(2))y^3$$
$$+ \; (4\phi_{ud}(2) - 4\phi_{ud}(0))x^2 - 2\phi_{ud}(1)xy + (2\phi_{ud}(2) - 2\phi_{ud}(0)$$
$$+ \; 8\phi_{ud}(3))y^2 + (\phi_{ud}(0) + 2 * \phi_{ud}(2) - 4 * \phi_{ud}(3))y$$
$$- \; \phi_{ud}(2) \; \} \tag{5.5b}$$

We need two starting functions $g_1(x, y, \tau)$ and $g_2(x, y, \tau)$, since there are two variables $x = \beta_1$ and $y = \beta_2$ [55].

$$g_1(x, y, \tau) = p_1^4 x^4 - q_1^4 \tag{5.6a}$$
$$g_2(x, y, \tau) = p_2^6 y^6 - q_2^6 \tag{5.6b}$$

where p_1, p_2, q_1 and q_2 are arbitrary complex numbers. The degrees of $g_1(x, y, \tau)$ and $g_2(x, y, \tau)$ are determined from the maximum degree of $h_1(x, y, \tau)$ and $h_2(x, y, \tau)$, respectively. The total degree of the homotopy function is $6 \times 4 = 24$, which is corresponding to the number of solution paths to be tracked.

Figure 5.4 shows the solution trajectories of $x = \beta_1$ and $y = \beta_2$ starting from the combined roots of $g_1(x, y, \tau) = 0$ and $g_2(x, y, \tau) = 0$. The solution providing a global minimum MSE is found to be $(\alpha_0, \beta_1, \beta_2) = (-0.122, -0.357, -0.189)$ with MSE $\xi = 0.064$.

This simulation illustrates the complexity of using higher order HCM filters. The paths to be tracked are too numerous, resulting in high possibility of path merging. It is obvious that the probability of path merging is much larger in AHCM filtering where the paths fluctuate randomly. Consequently, more frequent usage of path merging avoidance strategy is required, resulting in a slower processing speed.

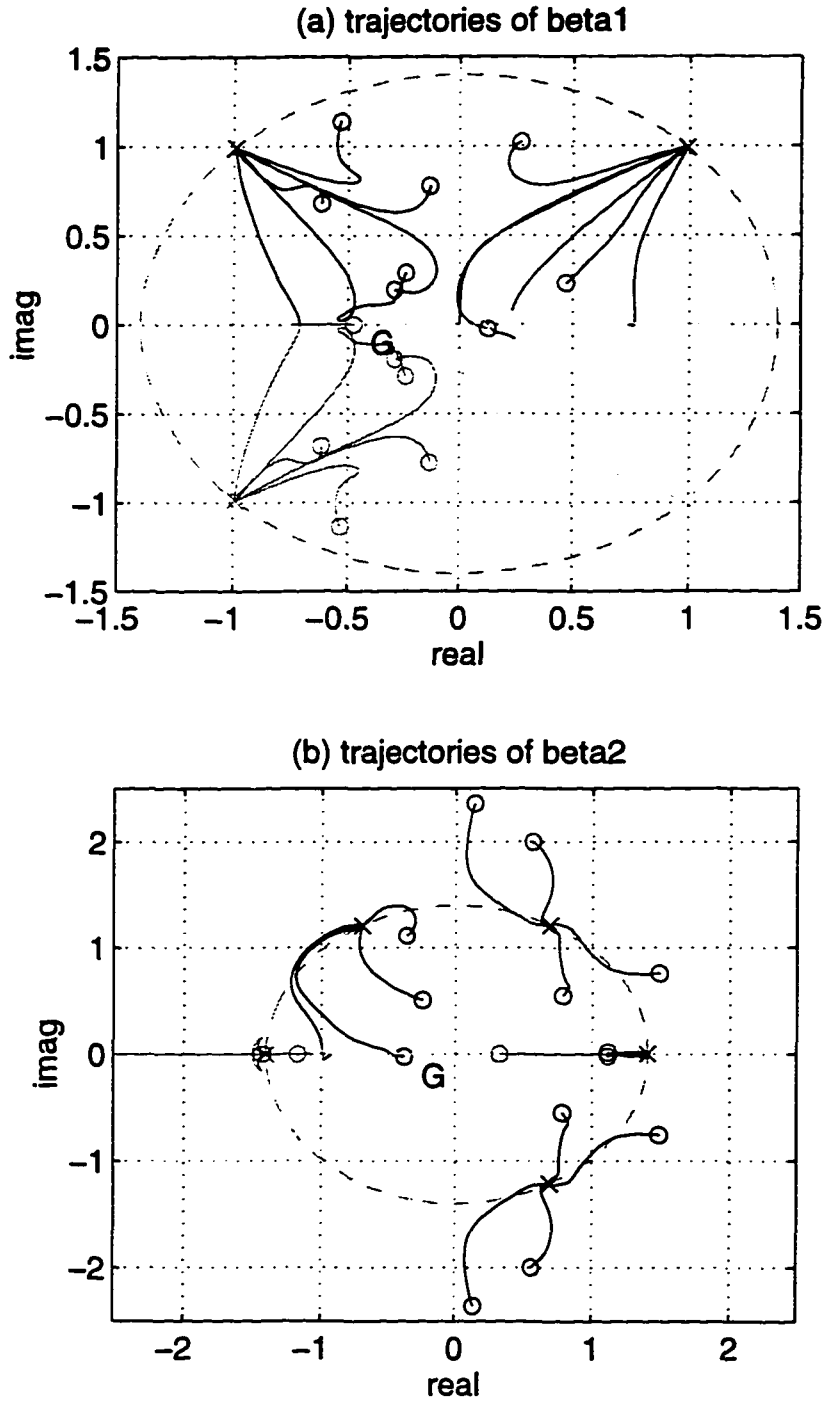

Figure 5.4 Solution trajectories of (a) β_1 and (b) β_2

AHCM: Adaptive Filtering

In this section, the same system identification examples are employed again in the simulations of AHCM IIR filters and its variations using a lower order model or under-modeling.

First-order IIR Filter

When the characteristic of the unknown system, $V(z)$, is (slowly or quickly) time-varying and non-stationary, we need a filter that adapts to the changes. In this case, a long-time observation of plant output signal is meaningless. Hence, the number of samples K, used in the instantaneous estimation of the coefficients $\hat{\phi}_{ud}(i,n)$, as given in Eq. (4.22), of polynomial equation is kept small.

As mentioned in Chapter 4, the AHCM IIR filter has four parameters: the order of polynomials L, the number of samples K, convergence parameter μ and the stepsize $\Delta\tau$. The accuracy of filter coefficients is largely dependent on the selection of L. The stepsize $\Delta\tau$ controls the convergence rate of the filter. $\Delta\tau$, K and μ also affect the smoothness of solution paths. The AHCM filtering is simulated for different values of these parameters with the same plant model used in the first-order non-adaptive filter.

- Number of samples K:

  Figure 5.5 shows the solution trajectories during AHCM filtering for $K = 5$ and $K = 20$. As K is increased, the solution paths become smoother. We see that from Figure 5.5 (a) and (b), a path may reach different solutions depending on the randomly changing input signal and the number of samples used for estimating $\phi_{ud}(n)$. The coefficients of the homotopy equation obtained from the instantaneous estimates of $\phi_{ud}(n)$, and the estimated values vary depending on the number of samples K.

- Convergence parameter μ:

  As mentioned in Chapter 4, the effect of K' and μ are mutually complementary on the smoothness of solution paths. The fluctuations in the solution paths for various values of μ is displayed in Figure 5.6. A smaller value of μ prevents the path from responding to abrupt changes in $\phi_{ud}(n)$, resulting in a smoother path tracking.

- Stepsize of homotopy parameter $\Delta\tau$:

  The stepsize used in the incrementing of τ uniquely decides the prediction solutions, resulting in different corrected solutions. Figure 5.7 shows the effect of $\Delta\tau$ on the smoothness of paths. The two plots (c) and (d) show more details of a path (path A) in finding the solution $\beta = 0.14 - 0.73i$ shown in plots (a) and (b).

Tracking Simulation

In the next simulation, the proposed algorithm is applied to track the changes of an unknown system. The transfer function of the unknown system chosen as

$$V_1(z) = \frac{0.05 - 0.4z^{-1}}{1 - 1.1314z^{-1} + 0.25z^{-2}} \tag{5.7}$$

is assumed to change to

$$V_2(z) = \frac{0.5 - 0.4z^{-1}}{1 - 1.1314z^{-1} + 0.25z^{-2}}, \tag{5.8}$$

after the modeled filter reaches an optimum state, $\tau = 1$. Notice that the MA coefficient is changed from 0.05 in $V_1(z)$ to 0.5 in $V_2(z)$. The MSE contour for $V_2(z)$ modeled with a one-pole AR filter is shown in Figure 5.8. The position of the global minimum of $V_2(z)$ has moved close to $\beta = 0.25$, from the global minimum position $\beta = 0.906$ of $V_1(z)$ shown in Figure 5.1.

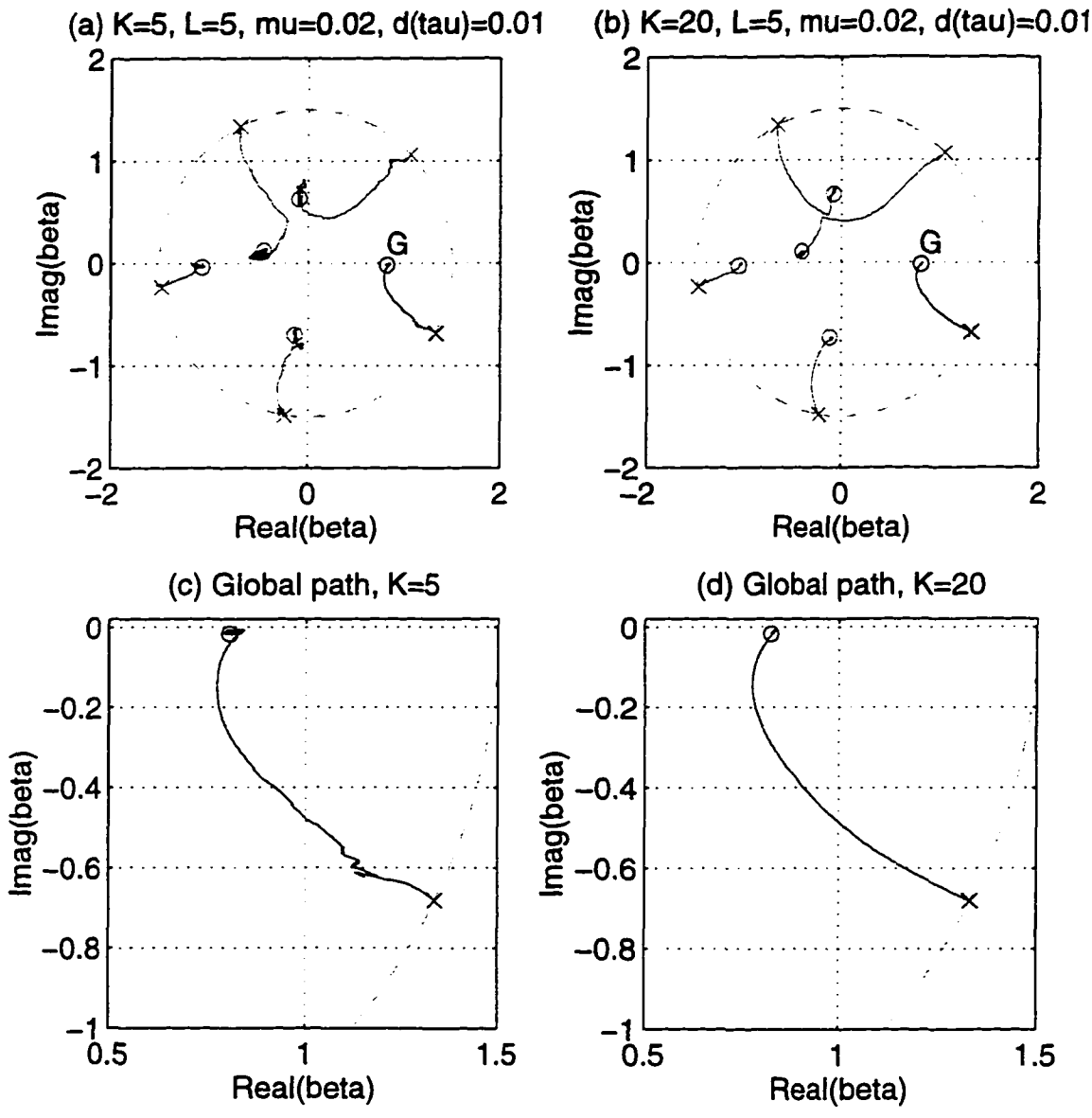

Figure 5.5 Solution trajectories of β (a) for $K = 5$, (b) for $K = 20$, (c) the detail of the path to the global minimum position for $K = 5$ and (d) for $K = 20$

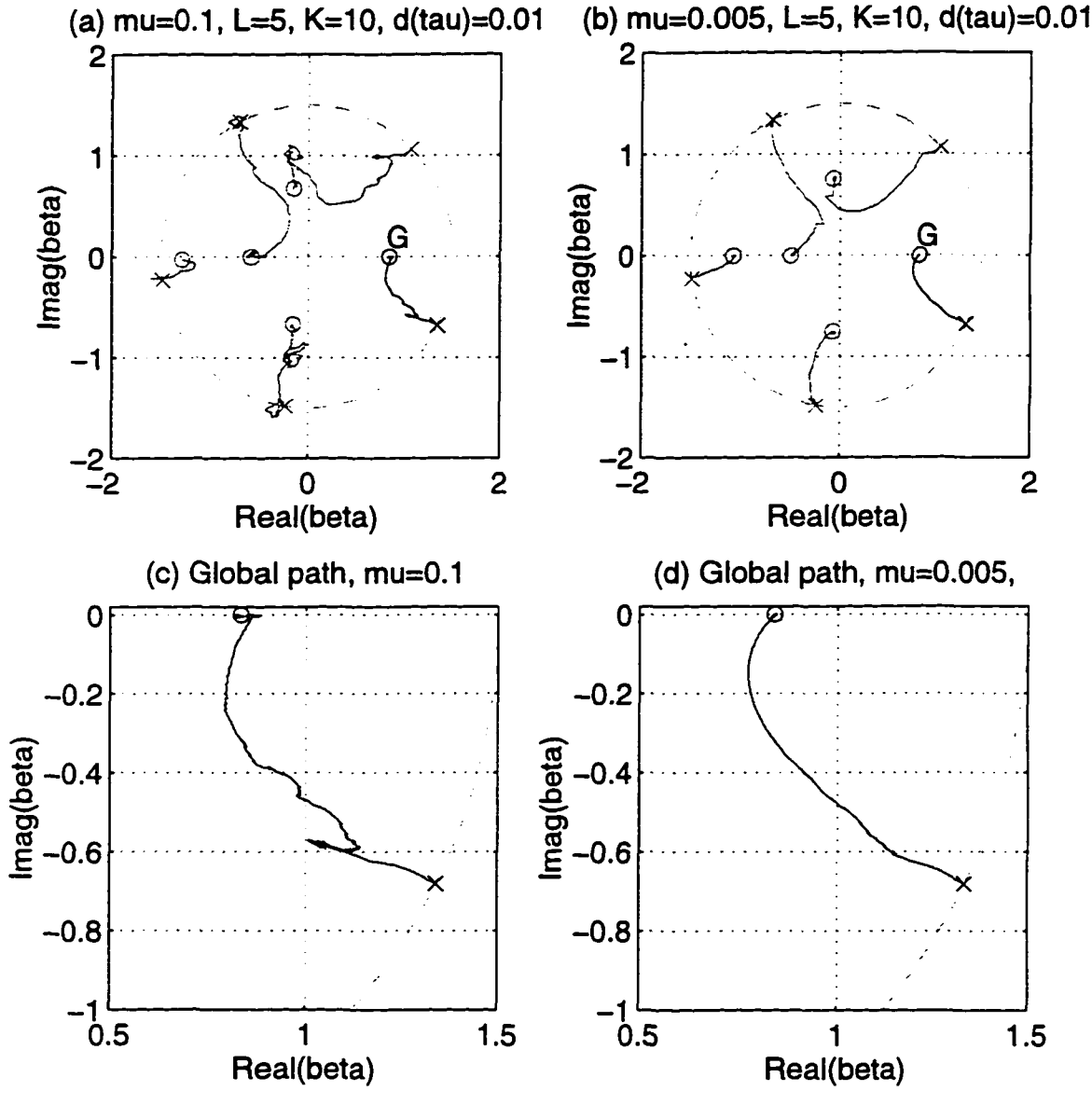

Figure 5.6 Solution trajectories of β (a) for $\mu = 0.1$, (b) for $\mu = 0.005$, (c) the detail of the path to the global minimum position for $\mu = 0.1$ and (d) for $\mu = 0.005$

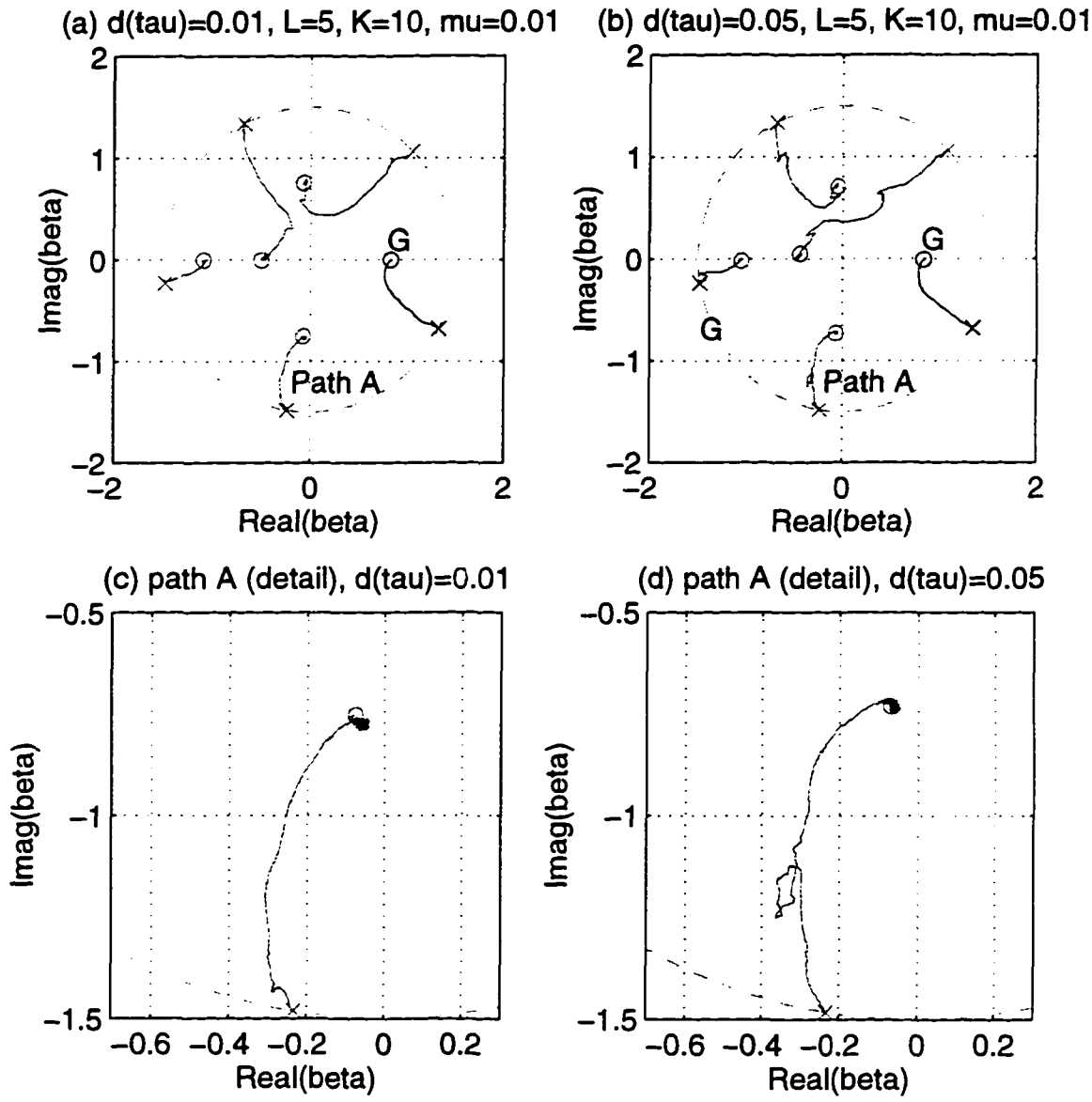

Figure 5.7 Solution trajectories of β (a) for $\Delta\tau = 0.01$, (b) for $\Delta\tau = 0.05$, (c) the detail of the path A for $\Delta\tau = 0.01$ and (d) for $\Delta\tau = 0.05$

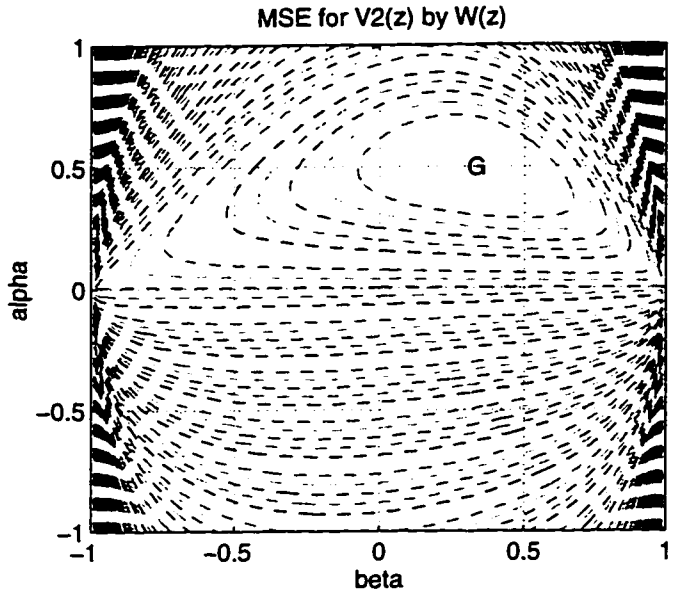

Figure 5.8 MSE plot for the changed system

Figure 5.9 shows the trajectories of β before (dotted lines) and after (solid lines) the system characteristic changed. It shows that the path converging to the global minimum position has switched. The original path that converged to the global minimum G_1 of $V_1(z)$ diverges, whereas the path, which was earlier at a local minimum of $V_1(z)$, converges to the global minimum position G_2 of $V_2(z)$. The value of τ remains unchanged at 1 during the tracking process.

AHCM-LMS Filters

The combination of AHCM and LMS algorithms for minimizing the MSE further is presented here. The AHCM-LMS filter is simulated using the one-pole filter to model the unknown system. Therefore, the initial starting filter coefficients for the LMS filter is given as $(\alpha, \beta) = (-0.285, 0.839)$ obtained earlier using the AHCM procedure. Figure 5.10 (a) shows that the AR filter parameter β converges to the ideal global minimum 0.906 quickly as iterations go on. The change in the corresponding MSE is also plotted

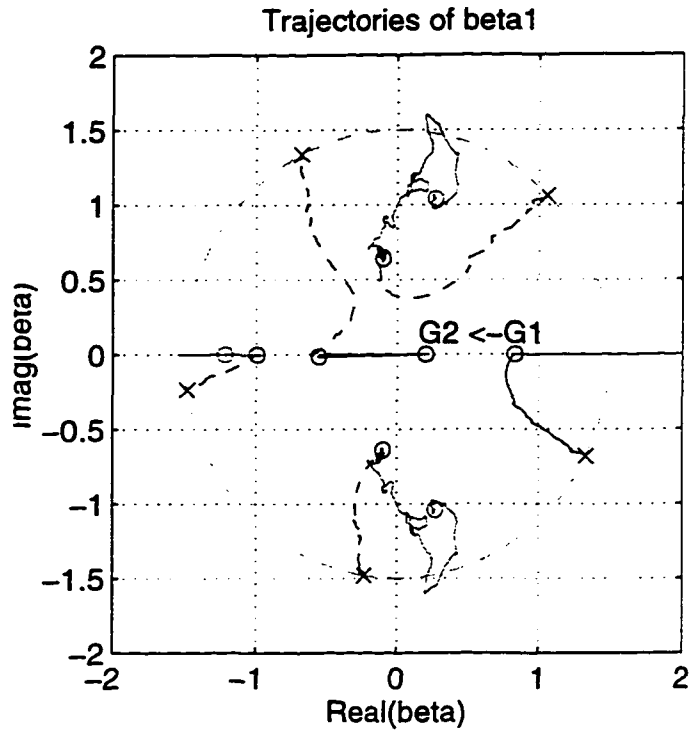

Figure 5.9 Change in the solution trajectories seeking a new global minimum position

in (b), confirming the discussions in Chapter 4.

MAHCM Filter

As seen in the simulation of a two-pole filter, the number of trajectories increase geometrically with the number of poles of the filter. As explained earlier, the high path density, shown in Figure 5.11, increases the possibility of path merging and consequently requires a small value of $\mu(= 0.002)$ and a large $K(= 20)$. However. a small μ and large K delay the response of the AHCM filter preventing it from adapting quickly to changes in the unknown system. The large number of solution paths, which is 24 in this example, is enough to offset the advantages of IIR filtering. As explained in Chapter 4, this problem can be overcome using an MAHCM.

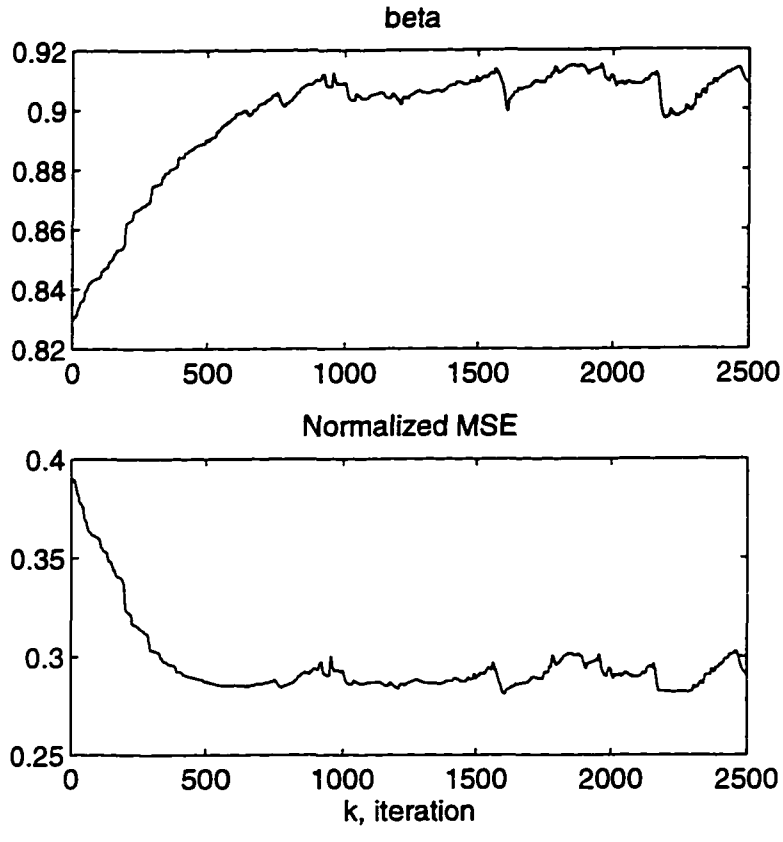

Figure 5.10 Changes in (a) $\beta(k)$ and (b) $MSE(k)$

In the simulation of the MAHCM filter, a one-pole AHCM filter is employed for each stage of the MAHCM filter. The plant model is picked to be equal to that of the first-order AHCM filter simulation presented earlier.

$$V(z) = \frac{C(z)}{D(z)} = \frac{0.05 - 0.4z^{-1}}{1 - 1.1314z^{-1} + 0.25z^{-2}} \tag{5.9}$$

The input signal of the second stage AHCM filter, AHCM2, is $u(n)$, and the desired signal $d_2(n)$ is obtained directly from $e_1(n) = d_1(n) - y_1(n)$. The second AHCM filter is represented by the transfer function

$$W_2(v) = \frac{\alpha_2}{1 - \beta_2} \tag{5.10}$$

Figure 5.12 shows the trajectories of the β_2, where the global minimum is found

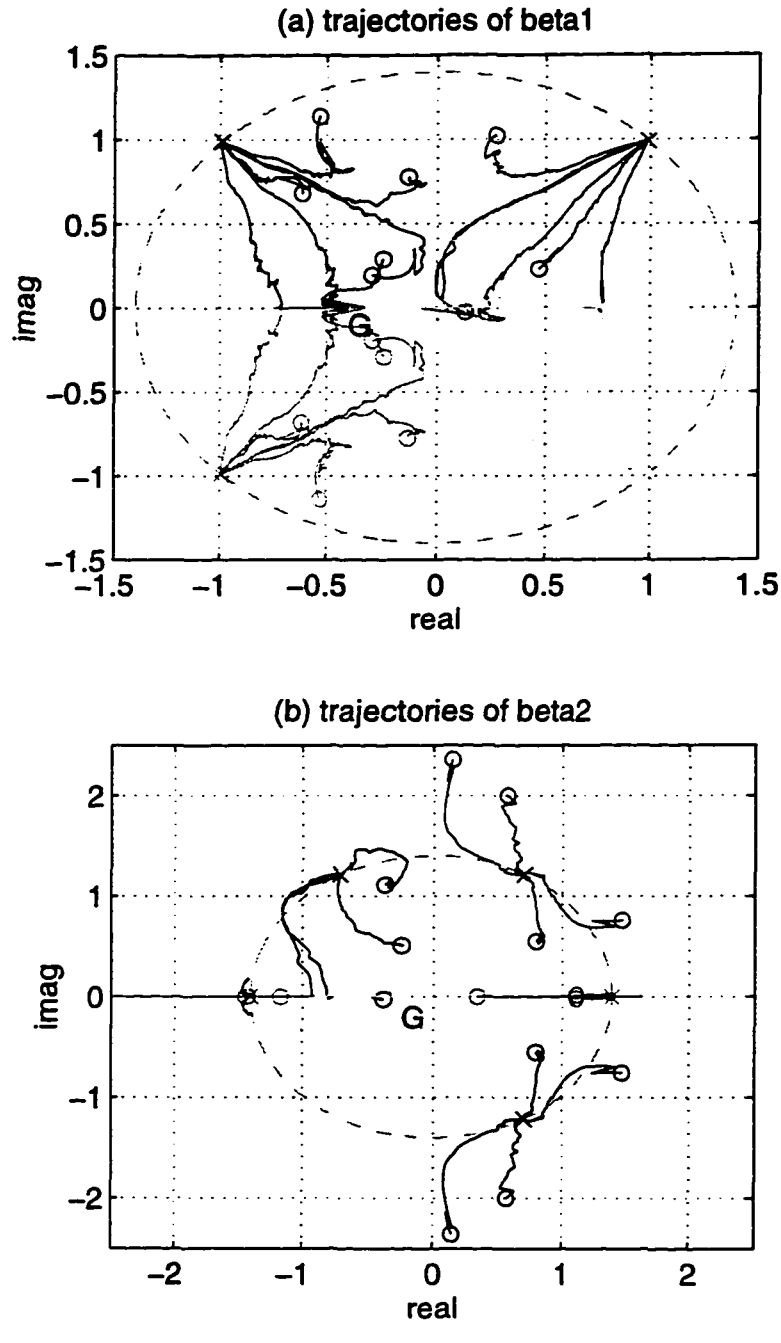

Figure 5.11 Solution trajectories of (a) β_1 and (b) β_2

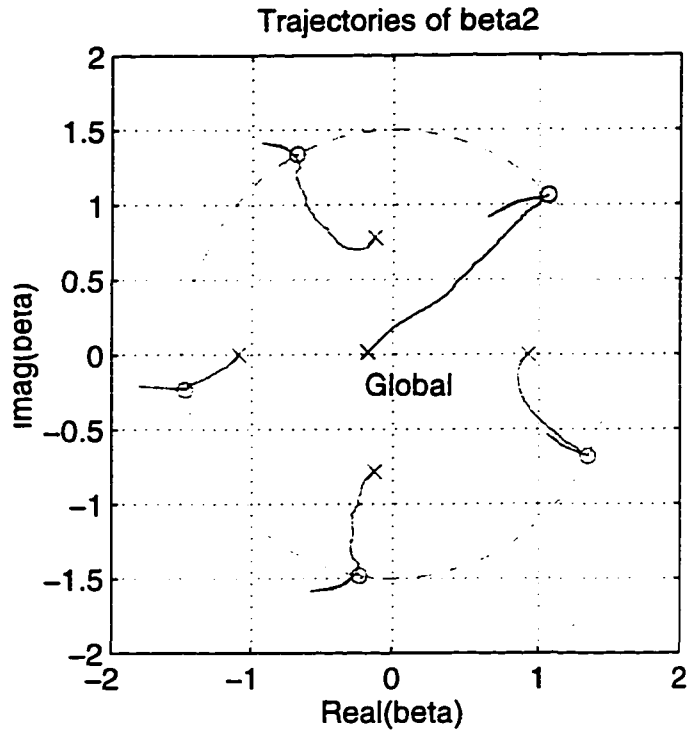

Figure 5.12 Solution trajectories of β_2 of $W_2(z)$

around -0.19.

The combined output signal $y_1(n)+y_2(n)$ is compared to the output of the first stage output $y_1(n)$ and desired signal $d_1(n)$ in Figure 5.13 (a). The MSE achieved with the two-stage MAHCM (even without the LMS procedure) shows significant improvement in performance as seen in Figure 5.13 (b). The desired signal of the AHCM2 $d_2(n) = e_1(n)$ is plotted along with the output signal $y_2(n)$ in Figure 5.13 (b).

Figure 5.14 shows a comparison of the impulse function of the unknown system and the filter impulse response. The filter impulse response becomes closer to the system impulse response as the number of stages increases. Notice that no more improvement in the filter impulse response can be achieved after the third stage. This is because the order of the filter exceeds the order of the system after the third stage.

The MSE calculated from a thousand time observations of the filter input and output

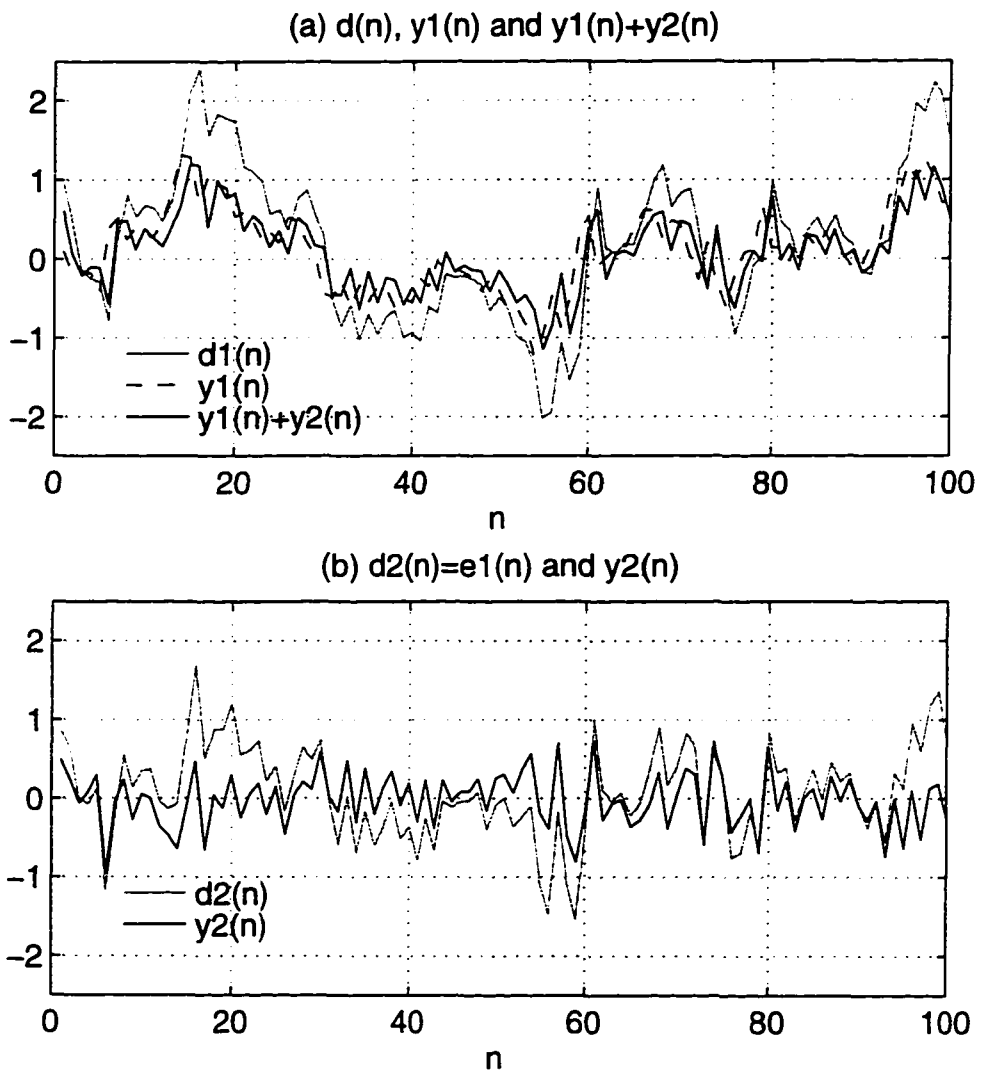

Figure 5.13 Comparisons of (a) $d(n)$, $y_1(n)$ and $y_1(n)+y_2(n)$ (b) $d_2(n)=e_1(n)$ and $y_2(n)$

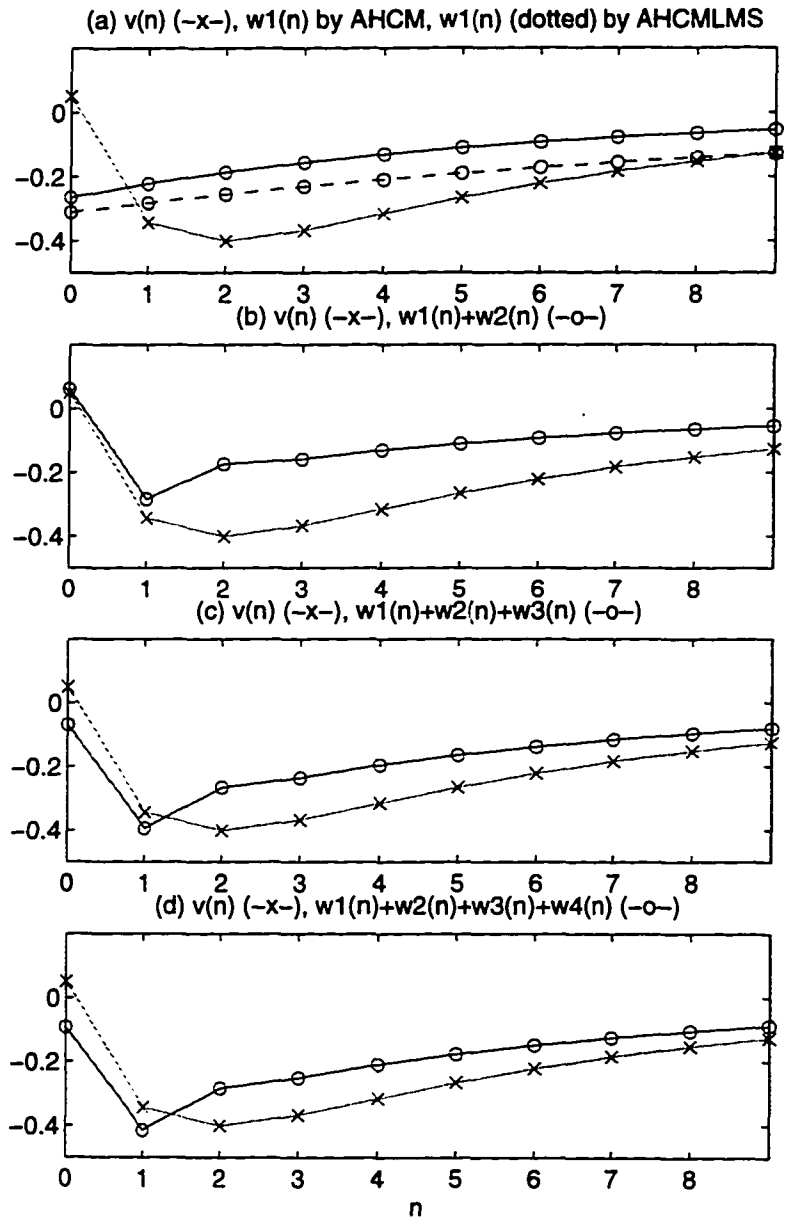

Figure 5.14 Impulse response of the unknown system and filter for stage number (a)$N = 1$, (b) $N = 2$, (c) $N = 3$ and (d) $N = 4$.

signals are listed in Table 5.2. The total MSE is achieved by connecting the filters in each stage. The MSE is obviously improved when the number of stages increases.

Table 5.2 Estimated MSE at global minimum, α, β by MAHCM IIR filtering

Stage no. N	α	β	Total MSE
1 (AHCM)	-0.264	0.839	0.331
1 (AHCM-LMS)	-0.311	0.906	0.218
2 (AHCM)	0.325	-0.193	0.085
3 (AHCM)	-0.131	0.840	0.072
4 (AHCM)	-0.023	0.871	0.082

6 ADAPTIVE NOISE CANCELLATION

In this chapter, the AHCM filtering technique is applied to a real world problem in nondestructive evaluation (NDE). The problem considered is a noise cancellation application of adaptive filters. One-dimensional ultrasonic signals in general are heavily corrupted by grain noise due to the scattering from material grain boundaries. The detection of a defect or a crack signal in titanium parts is often hindered by grain noise. In an effort to enhance the signal-to-noise ratio (SNR) using an AHCM filter, some assumptions on auto- and cross-correlation of grain noise and defect signals are made.

Grain Noise Reduction in Ultrasonic Non-Destructive Evaluation

In ultrasonic nondestructive evaluation [67], the detection of small defects is often limited by coherent scattering from boundaries of material microstructures called grains. Since the grains are usually randomly distributed in a material, the grain noise can be modeled as a stochastic process characterized by statistical properties. Many signal processing techniques have been proposed to increase the detectability of the small defect signals buried in grain noise. Some of the successful techniques [68] [69] [70] are based on the fact that the attenuation of grain noise is frequency dependent.

In recent papers, Zhu et al. [71] and Chiou et al. [72] proposed a new method utilizing an adaptive filtering technique to minimize the grain noise. The underlying idea of this method is that the desired target (defect) signal and the grain noise vary in

different ways when there is a small change in the position of the ultrasonic transducer. For example, the two ultrasonic signals will both contain uncorrelated contributions due to grain noise, but in the presence of a defect, the defect contributions will be correlated.

The technique uses an LMS finite impulse response (FIR) adaptive filter to perform the noise cancellation. However, application results of this method reveal that the use of a FIR adaptive filter requires a long convergence time before reaching an optimal state to track the changes in a signal. Therefore, small defects appearing near the beginning of the data stream are not likely to be detected.

The following sections describe the performance of the proposed filter structure (the AHCM filter) on the noise cancellation application in ultrasonic NDE.

Adaptive Filtering for Grain Noise Cancellation

The noise cancellation filtering scheme [13] used here is illustrated in Figure 6.1. In this figure, the reference signal and the primary input signal are obtained from two adjacent positions of the ultrasonic transducer.

The scheme shown in Figure 6.1 for grain noise cancellation is the variation of conventional noise cancellation explained in Chapter 2. In the conventional noise cancellation scheme, first, the information-bearing signal component of the primary input signal is not detectable in the reference input signal. Secondly, the reference input signal, which is assumed to be a noise-only signal, is highly correlated with the noise component of the primary input signal. Thirdly, the desired output signal is obtained from the error between the primary input signal and filter output to the reference input signal. That is, the desired output signal is obtained by subtracting correlated noise from the primary input signal, where the correlated noise is obtained by filtering (or, delaying) the reference input signal. It should be noted that when the noise-only reference input signal is perfectly uncorrelated with the noise component in the primary input signal.

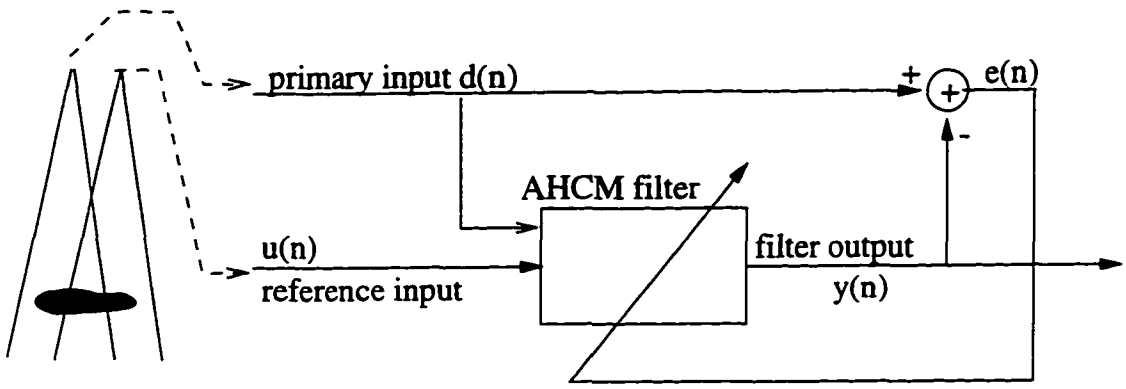

Figure 6.1 Adaptive filtering configuration for noise cancellation

the adaptive filter "switches itself off" resulting in a zero value of the filter output [12].

However, in the grain noise problem, the noise in the primary input and reference input signals are usually uncorrelated. However, correlated information-bearing target echoes exist in both input signals. Besides, the noise-free output signal is observed directly from the filter output, and not from the error signal. Consequently, we can say that the adaptive filter operates in the switch-off mode when both inputs, contain only grain noise components which are uncorrelated with each other. Therefore, the filter output is suppressed to be zero. When correlated target echoes exist in both input signals simultaneously with a small time delay, the filter operates in the identification mode, so that the filter output signal begins to resemble the primary input signal.

The noise cancellation concept can be described better through an error function analysis. Assume that the primary input signal, $d(n)$, consists of a target signal $s_d(n)$ and noise $n_d(n)$.

$$d(n) = s_d(n) + n_d(n) \tag{6.1}$$

And, the reference input signal is expressed as

$$u(n) = s_u(n) + n_u(n) \tag{6.2}$$

Suppose the noise signals $n_d(n)$ and $n_u(n)$ are uncorrelated with both $s_d(n)$ and $s_u(n)$, and the $s_u(n)$ is correlated with $s_d(n)$.

The mean squared error (MSE) between the filter output $y(n)$ and $d(n)$ is given by

$$\begin{aligned} E[e^2(n)] &= E[(d(n)-y(n))^2] && (6.3a)\\ &= E[((s_d(n)-y(n))+n_d(n))^2] && (6.3b)\\ &= E[(s_d(n)-y(n))^2+n_d^2(n)+2n_d(n)(s_d(n)-y(n))] && (6.3c) \end{aligned}$$

The filter output $y(n)$ can be expressed as

$$y(n) = w(n) * u(n) = w(n) * s_u(n) + w(u) * n_u(n) \qquad (6.4)$$

where $w(n)$ is the impulse response of the filter. Then, the MSE is

$$\begin{aligned} E[e^2(n)] &= E[\ \{d(n)-y(n)\}^2\ ] && (6.5a)\\ &= E[\ \{\ (s_d(n)+n_d(n))\ -\ (w(n)*s_u(n)+w(u)*n_u(n))\ \}^2\ ] && (6.5b)\\ &= E[\ \{\ (s_d(n)-w(n)*s_u(n))\ +\ (n_d(n)-w(u)*n_u(n))\ \}^2\ ] && (6.5c)\\ &= E[\ (s_d(n)-w(n)*s_u(n))^2\ +\ (n_d(n)-w(u)*n_u(n))^2 \\ &\quad -2(s_d(n)-w(n)*s_u(n))(n_d(n)-w(u)*n_u(n))\ ] && (6.5d)\\ &= E[\ (s_d(n)-w(n)*s_u(n))^2 \\ &\quad +(n_d^2(n)+(w(u)*n_u(n))^2\ -\ 2n_d(n)(w(u)*n_u(n)) \\ &\quad -2(s_d(n)-w(n)*s_u(n))(n_d(n)-w(u)*n_u(n))\ ] && (6.5e) \end{aligned}$$

When the filter is optimized, the mean square error is minimized. For instance, if $s_u(n)$ is a replica of $s_d(n)$ with a time delay, the filter minimizes the first term by finding the delay time, and, consequently, the first term vanishes. The second and third term will remain as the minimum error of the filter. The last two terms are zero because the noise and target signals are assumed to be uncorrelated. Consequently, the filter, in the optimal state, finds $w(n)$ which minimizes the error $s_d(n)-w(n)*s_u(n)$, where $s_d(n)$ and

$s_u(n)$ are obtained from two adjacent transducer positions. In the absence of defects, the filter is optimized to minimize the error between the noise signals $n_d(n) - n_u(n)$. Since the noise signals are uncorrelated, the filter output signal is close to zero.

Ultrasonic NDE Signals and Grain Noise

In the conventional pulse-echo ultrasonic nondestructive testing of a sample [67], such as an aircraft component, an ultrasonic transducer sends an ultrasonic wave in the the object and receives the reflections from discontinuities in the material. The received energy is converted into an electric signal by the transducer, resulting in a one-dimensional signal, namely an A-scan signal. A C-scan image of ultrasonic NDE signals is obtained by taking maximum values of multiple A-scan signals obtained from a surface area of the object.

The C-scan image shown in Figure 6.2 is from the ultrasonic NDE inspection of a flat metal plate sample. Each pixel corresponds to the maximum value of the A-scan signal acquired at each transducer position. The sample contains two artificial flat bottomed holes (FBH) on its back-surface for simulating hidden defects in the sample. The flat metal plate is placed on another plate. The bright circles near (30,30) and (90,30) represent indications of the FBHs. The highly granular microstructure of the material generates strong interference noise in the ultrasonic signal. Other less bright circles in the image originate from either grain structure or the back plate.

Figure 6.3 compares (a) the two A-scan signals without echoes from FBHs, i.e., pure grain noise, and (b) two signals with echoes from a FBH, located 0.5" below the surface. The signals are acquired using a 7.5 MHz wideband transducer. Each pair of signals are acquired from two adjacent locations such that both A-scans contain the same target indications. The A-scan signals of pure grain noise show no correlation while the signals from flaws exhibit correlated echoes with higher amplitude. When the echoes from the

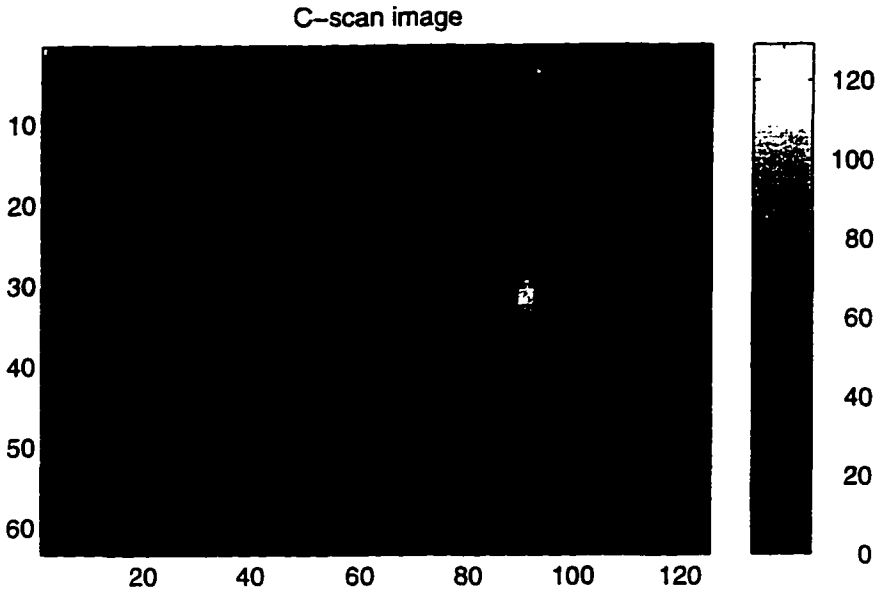

Figure 6.2 The C-scan image containing crack and grain signals

defect are not large relative to the magnitude of grain noise, the detection of the crack signal becomes very difficult.

The correlation property of the grain noise is highly dependent on the distance between the positions of the transducer. For the noise cancellation, the grain noise in the desired signal $d(n)$ and filter input signal $u(n)$ are required to be uncorrelated. It is observed that, for the selected sample, the grain noise is not strongly correlated with each other when they are separated by more than 5 pixels in the C-scan image. Two pure grain noise (no defect) signals satisfying this distance criteria were picked, and the normalized autocorrelations and cross-correlations are estimated and plotted in Figure 6.4. The cross-correlation function in (b) reveals that the grain noise signals are sufficiently uncorrelated to validate the assumption. The autocorrelation property shown in (a) is estimated to check its closeness to an impulse, which allows the direct use of the adaptive homotopy continuation method filtering technique. The AHCM filtering algorithm derived for a system identification problem requires its input signal to have an

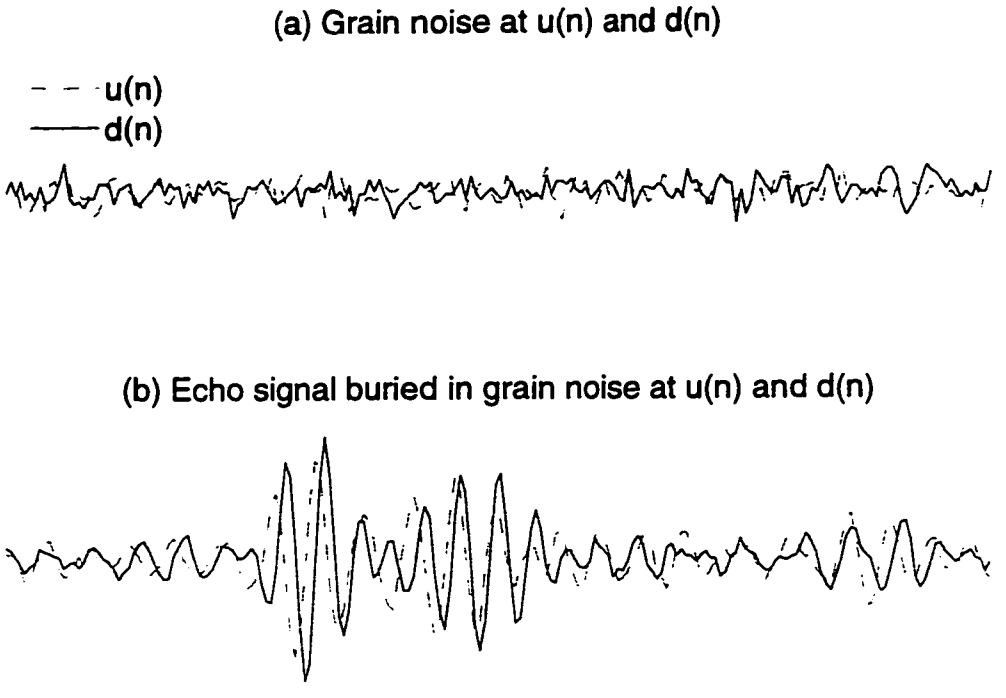

Figure 6.3 Comparison of the signals

impulse autocorrelation function. The estimated autocorrelation function is very similar to an impulse with decreasing sidelobe at multiples of the transducer frequency.

Experiment Results And Discussions

The AHCM IIR filtering algorithm is applied to reduce the grain noise in the ultrasonic A-scan signals described earlier.

- Experimental I. two defect-free signals

  The algorithm was first applied on the two pure grain noise signals, one used as the primary input signal and the other as the reference input signal, as presented in the schematic of Figure 6.1. The signals chosen from the defect-free area are confirmed to have the required correlation properties. With $\Delta\tau$ for the homotopy parameter chosen as 0.01, the filter converges to an optimal state in only one

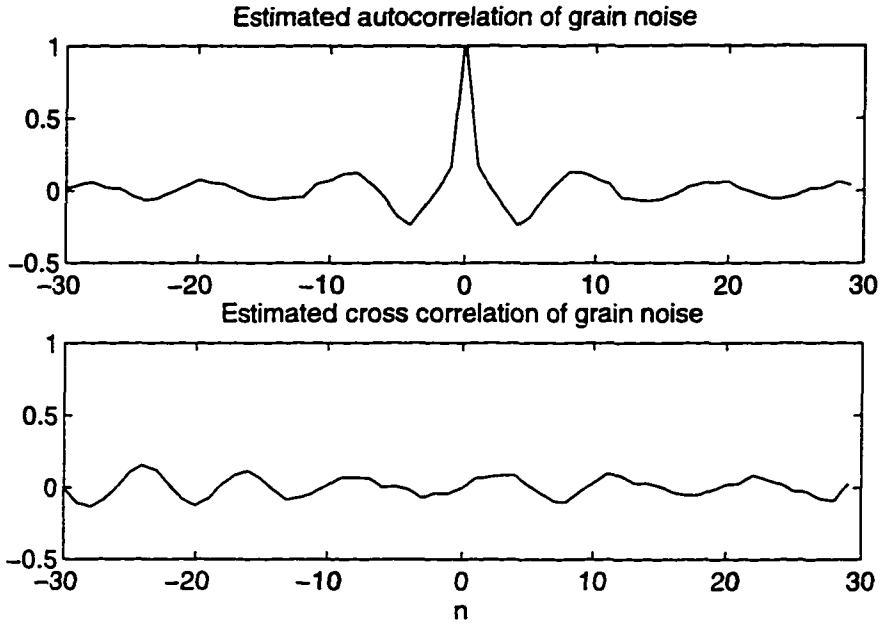

Figure 6.4 Auto-correlation and cross-correlation of grain noise

hundred iterations. A one-pole filter is used. Figure 6.5 shows the trajectory of the pole (β_1) as a function of iteration steps. It shows the β_1 changes in time to adapt the signal changes.

The results of experiment I are presented in Figure 6.6. The plot of the filter output shown in (c) demonstrates a successful noise cancellation. The filter output when the AHCM filter is in a transient state ($\tau < 1$) is assumed to be all-pass. The indication in the last part of the filter output is from the boundary between the two flat plates where the signals are inherently correlated. Consequently, the filter performance is degraded in this position. The input signal and its noise-free version (filter output) are compared in detail in (d), showing an obvious improvement in signal-to-noise ratio. The improvement in signal-to-noise ratio is more than 10dB. The SNR is estimated by a ratio of the mean of squared amplitude of the target echo signal, for the duration of the target echo, to that of the grain noise.

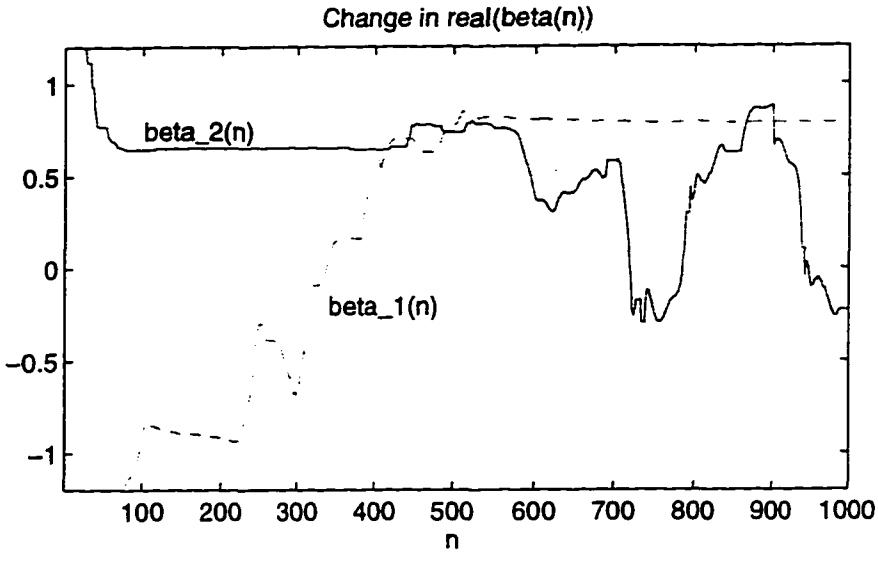

Figure 6.5 Trajectories of β for no-echo signal and echo signal

- Experiment II. two defect signals

  In the second experiment, two signals containing echoes from a FBH crack were selected as the input of the AHCM filter. The trajectory of pole (β_2) is plotted in Figure 6.5. The same stepsize $\Delta\tau = 0.01$ is used. The results of experiment II are plotted in Figure 6.7. Even though the indication of the defect is clearly visible before filtering, it is shown that the AHCM filtering further increases signal-to-noise ratio. If a small echo from a defect buried in grain noise exists, the filtering process can potentially help in detecting it.

The results show the AHCM filtering successfully reduces grain noise and results in an enhanced signal-to-noise ratio. Besides, the inherent quick convergence rate makes the AHCM filter superior to LMS based adaptive filtering algorithms for eliminating grain noise.

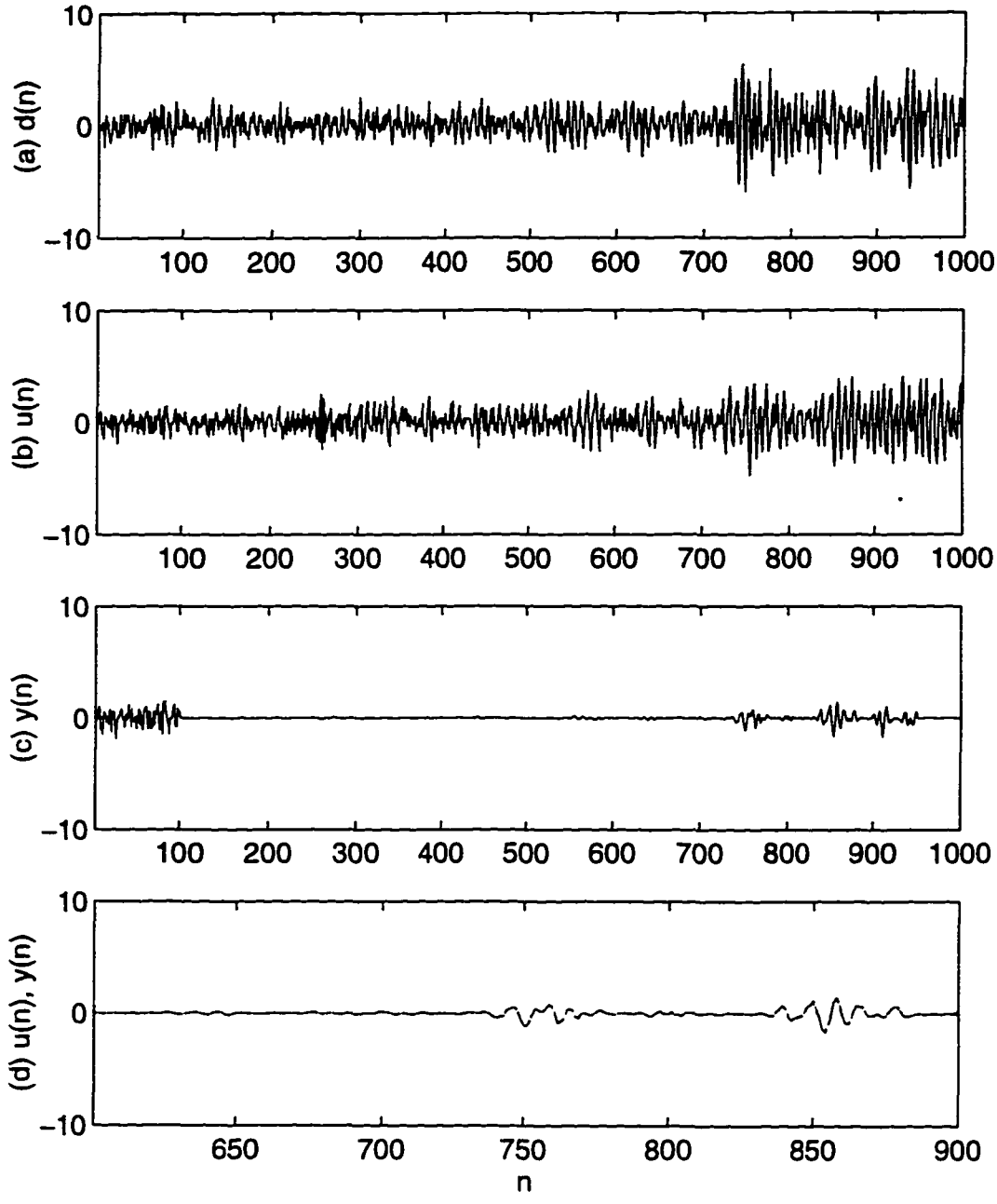

Figure 6.6 Filtering results of two no-echo signals: (a) desired signal $d(n)$ (b) input signal $u(n)$ (c) filter output signal $y(n)$, and (d) $y(n)$ and $u(n)$ in detail

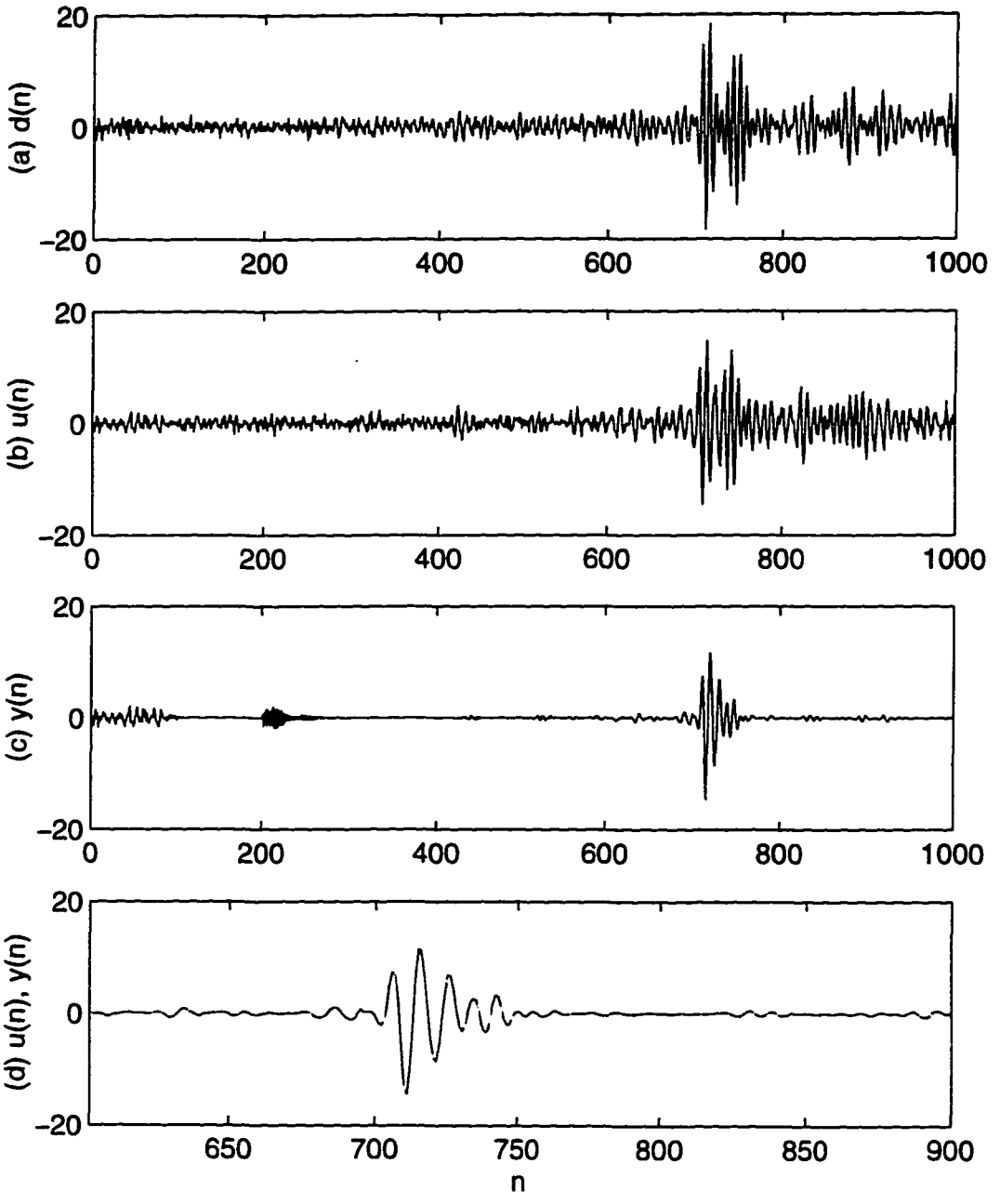

Figure 6.7 Filtering results of two echo signals: (a) desired signal $d(n)$ (b) input signal $u(n)$ (c) filter output signal $y(n)$, and (d) $y(n)$ and $u(n)$ in detail

7 CONCLUSIONS

The motivation for using adaptive IIR filters was first described and a review of existing techniques for filter design was presented. The major drawbacks of existing techniques in adaptive IIR filtering were identified as (i) convergence to a local minimum and (ii) instability. A new algorithm for adaptive IIR filtering has been developed and its performance has been demonstrated on a number of benchmark problems.

The proposed algorithm is based on the homotopy continuation method (HCM) which is a solution exhaustive technique for solving nonlinear polynomial systems by tracking the known solutions of a simple system to the unknown solutions of the desired system. A basic path tracking, prediction-correction algorithm was also described. The HCM and path tracking were then modified for the application to the adaptive IIR filtering problem. This involves the formulation of the IIR filter design problem using a system of polynomial equations with time-varying coefficients. The conventional HCM is then modified to adapt to the time-varying polynomial coefficients, resulting in a new adaptive IIR filtering algorithm called an adaptive HCM (AHCM) filtering algorithm. Several parameters, L, K, μ, and $\Delta\tau$, controlling the iterative process were introduced and the parametric effects on the performance of the algorithm were presented.

The major drawbacks of the proposed algorithm were identified as (i) path merging and (ii) infinitely growing number of paths. These difficulties were addressed by introducing variations of the AHCM algorithm such as AHCM-LMS and MAHCM algorithms. The AHCM-LMS filtering algorithm has been proposed to solve the problem of an infinitely growing number of paths, where the concept of conventional least mean

square adaptive filter is combined with the AHCM filtering algorithm. It was shown that the possibility of path merging could be greatly reduced by the MAHCM filter which was constructed as a cascade of low-order AHCM filters.

The overall algorithm was evaluated on univariate and multivariate systems of polynomial functions. The algorithm was clearly shown to have achieved the main objectives namely convergence to a global minimum and stability. For further investigation of the proposed algorithm, the filtering technique was applied to a real world problem in noise cancellation. The algorithm clearly demonstrated a large signal-to-noise enhancement in ultrasonic NDE signals corrupted by uncorrelated noise due to scattering from grain boundaries.

Future Work

Most of the efforts in this study were concentrated on solving the local minimum convergence problem. A balanced effort for solving the instability problem is also important. An investigation of additional variations of the proposed filtering algorithm is necessary for avoiding instability. For example, the concept of lattice structure filters can be combined with the AHCM algorithm for further improvement of stability characteristics.

Even though the MAHCM filter operates with reduced computational complexity, there is still a need for reducing the computation in the basic AHCM procedure. While maintaining the AHCM structure, further simplification on the prediction-correction operation can be an interesting study. Also, the overall procedure of path tracking is parallel in nature. A parallel implementation of the filtering algorithm can speed up the convergence times significantly.

APPENDIX INDEPENDENCE PRINCIPLE

The proper selection of a starting function, when a target polynomial is given, is discussed here using a simple example. It is shown that badly chosen coefficients of the starting function cause singular points, resulting in path merging during homotopy parameter τ increases from 0 to 1. A simple rule to avoid this is presented.

Consider a second-degree polynomial $f(x)$ represented as

$$f(x) = x^2 + ax + b = 0 \tag{A.1}$$

The homotopy function $h(x)$ to solve $f(x) = 0$ is given as

$$h(x, \tau) = (1 - \tau)g(x) + \tau f(x) = 0 \tag{A.2}$$

where the starting function $g(x)$ can be chosen as,

$$g(x) = x^2 - q^2 \tag{A.3}$$

In Chapter 2, it is briefly mentioned that q must be "independent" of the coefficients of $f(x)$ for proper path behavior.

A counter-example where q is improperly chosen is presented to give a clue to understand the meaning of the "independence choice", first. Let $a = -4$ and $b = 1$ for $f(x)$, then

$$f(x) = x^2 - 4x + 1 = 0 \tag{A.4}$$

and, select $q = \pm j = \pm\sqrt{-1}$ for $g(x)$, so

$$g(x) = x^2 + 1 \tag{A.5}$$

Then, the homotopy function is

$$\begin{aligned} h(x,\tau) &= (1-\tau)g(x)+\tau f(x) && \text{(A.6a)} \\ &= (1-\tau)(x^2+1)+\tau(x^2-4x+1) && \text{(A.6b)} \\ &= x^2-4\tau x+1 && \text{(A.6c)} \end{aligned}$$

The homotopy function has a multiplicity when $\tau = 0.5$.

$$h(x,\tau=0.5) = x^2-2x+1 = (x-1)^2 = 0 \qquad \text{(A.7)}$$

Therefore, the paths starting from $+j$ and $-j$ are inevitably merging when τ reaches 0.5, which is a non-path behavior. Generally, this undesirable problem occurs when the homotopy function is "singular" at the position. That is, the derivative of $h(x,\tau)$ is zero at the position where $h(x,\tau)$ is zero. In this example, the singular position is at $(x,\tau) = (1,0.5)$.

$$h(x=1,\tau=0.5) = x^2-2x+1|_{x=1} = (x-1)^2|_{x=1} = 0 \qquad \text{(A.8)}$$

and

$$\frac{dh}{dx}(x=1,\tau=0.5) = 2(x-1)|_{x=1} = 0 \qquad \text{(A.9)}$$

The singular position can be avoided by choosing q independent of coefficients a and b. In this example, coefficient $-q^2$ of $g(x)$ is identical to the coefficient b of $f(x)$. Even though this has happened unintentionally, the result shows the chosen q is not independent of the coefficients of $f(x)$.

Consider the homotopy function again

$$\begin{aligned} h(x,\tau) &= (1-\tau)g(x)+\tau f(x) && \text{(A.10a)} \\ &= (1-\tau)(x^2+q^2)+\tau(x^2+ax+b) && \text{(A.10b)} \\ &= x^2+a\tau x+\tau b-(1-\tau)q^2 && \text{(A.10c)} \end{aligned}$$

Then,

$$\frac{dh}{dx}(x,\tau) = 2x + a\tau = 0 \tag{A.11}$$

therefore, $x = -a\tau/2$. Substituting this value into Eq. (A.10c) yields

$$-a^2\tau^2 + 4(b+q^2)\tau - 4q^2 = 0, \tag{A.12}$$

To avoid the singular point, q must be selected such that the above condition does not hold. One simple choice of q to avoid the singular problem is a complex number $c + dj$, requiring that c and d are nonzero. When a and b are real numbers, the choice of q to be a complex number $q = c + dj, c \neq 0, d \neq 0$ always satisfies the condition.

Morgan [55] had stated the independence selection of q as follows:

"But if both real and imaginary parts of q are chosen using a random number table, as we do in a practical application, it is highly unlikely that any special relationship between q and the coefficients of $f(x)$ will hold. This assumes that $f(x)$'s coefficients are not directly derived from q."

BIBLIOGRAPHY

[1] L. Ljung and T. Soderstrom, *Theory and Practice of Recursive Identification*. M.I.T. Press, Cambridge, MA, 1983

[2] T. Soderstrom, and P. Stoica, "Some Properties of the Output Error Method", *Automatica*, vol. 18, pp. 93-99, 1982

[3] R. P. Gooch, *Adaptive Pole-zero Filtering: The Equation-Error Approach*. Ph.D Dissertation, Stanford University, Palo Alto, CA, 1983

[4] S. Marcos, O. Macchi and C. Vignat, "Unified Framework for Gradient Algorithms Used for Filter Adaptation and Neural Network Training", *International Journal of Circuit Theory and Applications*, vol. 20, pp. 159-200, 1985

[5] V. Solo and X. Kong, *Adaptive Signal Processing Algorithms: Stability and Performance*, Prentice-Hall, Englewood Cliffs, NJ, 1995

[6] O. Macchi. *Adaptive Processing: The Least Mean Squares Approach with Applications in Transmission*, John Wiley and Sons Ltd, New York, NY, 1995

[7] S. D. Sterns, "Error Surfaces of Recursive Adaptive Filters", *IEEE Transactions on Acoustics, Speech, Signal Processing*, vol. ASSP-29, pp. 763-766, 1981

[8] J. M. Mendel, *Discrete Technique of Parameter Estimation: The Equation Error Formulation*, Marcel Dekker. New York, NY, 1973

[9] J. J. Shynx, "Adaptive IIR Filtering", *IEEE Signal Processing Magazine*, vol. 6, pp. 4-21, 1989

[10] Phillip A. Regalia, *Adaptive IIR Filtering in Signal Processing and Control*, Marcel, Dekker, Inc., New York, NY, 1995

[11] K. J. Astrom and T. Soderstrom, "Uniqueness of the Maximum Likelihood Estimates of the Parameters of an ARMA Model", *IEEE Transactions on Automatic Control*, vol. 19, pp. 769-773, 1973

[12] Simon Haykin, *Adaptive Filter Theory*, 2nd Edition, Prentice-Hall, Englewood Cliffs, NJ, 1991

[13] B. Widrow, "Adaptive noise canceling: Principles and applications", *Proceedings of the IEEE*, vol. 63, pp. 1692-1716, 1975

[14] I. D. Landau, *Adaptive Control: The Model Reference Approach*, Marcel Dekker, New York, NY, 1979

[15] C. R. Johnson, Jr., "Adaptive IIR Filtering: Current results and open issues", *IEEE Transactions on Information Theory*, vol. IT-30, no. 2, pp. 237-250, 1984

[16] S. Horvath, Jr., "A new adaptive recursive LMS filter", *Digital Signal Processing*, Edited by V. Cappellini and A. G. Constantinides, Academic Press, New York, 1988

[17] H. Fan and M. Nayeri, "Counter Examples to Sterns' Conjecture on Error Surfaces of Adaptive IIR Filters", *Proceedings of IEEE Int. Conf. on Acoustics, Speech and Signal Processing*, New York, NY, April 11-14, 1988

[18] H. Fan and M. Nayeri, "On Error Surface of Sufficient Order Adaptive IIR Filters: Proofs and Counter Examples to a Unimodality Conjecture", *IEEE Transactions*

on Acoustics, Speech, and Signal Processing, vol. Assp-37, no. 9, pp. 1436-1442, 1989

[19] T. Soderstrom, "On the Uniqueness of Maximum Likelihood Identification", *Automatica*, vol. 11, no. 2, pp. 193-197, 1975

[20] B. Widrow, J. M. McCool, M. G. Larimore and C. R. Johnson, Jr, "Stationary and Nonstationary Learning Characteristics of the LMS Adaptive Filter", *Proceedings of the IEEE*, vol. 64, No. 8, pp. 1151-1162, 1976

[21] B. Widrow and S. D. Sterns, *Adaptive Signal Processing*, Prentice-Hall, Englewood Cliffs, NJ, 1985

[22] E. I. Jury, *Theory and Applications of the Z-transform Method*, Wiley, New York, NY, 1964

[23] S. A. Tretter, *Introduction to Discrete-Time Signal Processing*, Wiley, New York, NY, 1976.

[24] H. Fan and M. Doroslowacky, "On global convergence of Steiglitz-McBride adaptive algorithm", *IEEE Transactions on Circuits and Systems - II*, vol. 40, pp. 73-87, 1993

[25] J. B. Kenney and C. E. Rohrs, "The composite regressor algorithm for IIR adaptive systems", *IEEE Transactions on Signal Processing*, vol. 41, pp. 617-628, 1993

[26] Gyula Simon and Gabor Receli, "A New Composite Algorithm to Achieve Global Convergence", *IEEE Transactions on Circuits and Systems - II: Analog and Digital Signal Processing*, vol. 42, no. 10, pp. 681-684, 1995

[27] D. H. Crawford, R. W. Stewart and T. Toma, "Alternative and effective adaptive IIR filter structure", *Electronics Letters*, October, 1995

[28] M. Nayeri and W. K. Jenjins, "Alternate realizations to adaptive IIR filters and properties of their performance", *IEEE Transactions on Circuits and Systems - II: Analog and Digital Signal Processing*, vol. 36, pp. 485-496, 1989

[29] J. Shimizu, Y. Miyanaga and K. Tochinai, "A Cascade Lattice IIR Filter for Total Least Squares Problem", *IEICE Transactions on Fundamentals*, vol. E79-A, no. 8, pp. 1151-1156, 1996

[30] I. L. Ayala, "On a new adaptive lattice algorithm for recursive filters", *IEEE Transactions on Acoustics, Speech, and Signal Processing*, vol. ASSP-30, no.2, pp. 316-319, 1982

[31] H. Fan and W. K. Jenkins, "A new adaptive IIR filter", *IEEE Transactions on Circuits Systems*, vol. CAS-33, no. 10, pp. 939-947, 1986

[32] H. Fan, "Application of Benveniste's convergence results in a study of adaptive IIR filtering algorithms", *IEEE Transactions on Information Theory*, vol. 34, no. 4, pp. 692-709, 1988

[33] Phillip A. Regalia, "Stable and Efficient Lattice Algorithm for Adaptive IIR Filtering", *IEEE Transactions on Signal Processing*, vol. 40, no. 2, 1992

[34] P. L. Feintuch, "An adaptive recursive LMS filter" *Proceedings of the IEEE*, vol. 64, no. 11, pp. 1622-1624, 1976

[35] Qiang Ma and Colin F. N. Cowan, "Genetic algorithms applied to the adaptation of IIR filters", *Signal Processing*, vol. 48, pp. 155-163, 1996

[36] T. J. Lim and M. D. Macleod, "Adaptive Algorithms for Joint Time Delay Estimation and IIR Filtering", *IEEE Transactions on Signal Processing*, vol. 43, no. 4, pp. 841-852, 1995

[37] Jinhui Chao, Shinobu Kawabe and Shigeo Isujii, "A New IIR Adaptive Echo Canceler: GIVE", *IEEE Journal on Selected Areas in Communications*, vol. 12, no. 9, pp. 1530-1539, 1994

[38] H. J. W. Belt, A. C. den Brinker, and F. P. A. Benders, "Adaptive Line Enhancement Using a Second-order IIR Filter", *The 1995 IEEE International Conference on Acoustics, Speech, and Signal Processing, Conference Proceedings*, vol. 2, pp. 1444-1447, 1995

[39] D. H. Crawford, R. W. Stewart and E. Toma, "A Novel Adaptive IIR Filter for Active Noise Control", *The 1996 IEEE International Conference on Acoustics, Speech, and Signal Processing, Conference Proceedings*, vol. 3, pp. 1629-1632, 1996

[40] J. J. Shynk, "A complex adaptive algorithm for IIR filtering", *IEEE Transactions on Acoustics, Speech, and Signal Processing*, vol. ASSP-34, no. 5, pp. 1342-1344, 1986

[41] T. A. C. M. Classen, W. F. G. Meeklen brauker and J. B. H. Peck, "Effects on quantization and overflow in recursive digital filters", *IEEE Transactions on Acoustics, Speech, and Signal Processing*, vol. ASSP-24, pp. 517-529, 1976

[42] O. Macchi, "Common Formalism for Adaptive Identification in Signal Processing and Control", *Proceedings of the IEEE*, vol. 38, pp. 295-307, 1991

[43] T. Nakachi, K. Yamashita and N. Hamada, "2-D Adaptive Autoregressive Modeling Using New Lattice Structure", *IEICE Transactions on Fundamentals*, vol. E79-A, no. 8, pp. 1145-1150, 1996

[44] R. Seydel and V. Hlavacek, "Role of Continuation Method in Engineering Analysis", *Chemical Engineering Science*, vol. 42, no. 6, pp. 1281-1295, 1987

[45] K. Iba, H. Suzuki, M. Egawa and T. Watanabe, "Calculation of Critical Loading Condition with Nose Curve Using Homotopy Continuation Method", *IEEE Transactions on Power Systems*, vol. 6, no. 2, pp. 584-593, 1991

[46] N. Karmarkar, *new polynomial time algorithm for linear programming*, **Combinatorica 4**, 1984

[47] J. F. Brophy and P. W. Smith, *Prototyping Karmarkar's algorithm using MATH/PROTAN*, **Corections 5**, IMSL Corp. Houston, Texas, 1988

[48] S. S. Shurpalekar. *Homotopy Continuation Method for the Estimation of Signal Parameters*, MS thesis, Iowa State University, Ames, IA, 1993

[49] J. C. Chow, *Neural Networks Using Homotopy Continuation Methods*, MS thesis, Iowa State University, Ames, IA, 1991

[50] C. B. Garcia and W. I. Zangwill, "Determining All Solutions to Certain Systems of Nonlinear Equations", *Mathematics of Operations Research*, vol. 4, pp. 1-14, 1979

[51] C. B. Garcia and W. I. Zangwill, "Finding All Solutions to Polynomial Systems and Other Systems of Equations", *Mathematical Programming*, vol. 16, pp. 159-176, 1979

[52] David R. Kincaid and E. Ward Cheney, *Numerical analysis: mathematics of scientific computing*, Brooks/Cole Publishing Company, Pacific Grove, CA, 1991

[53] Terrence J. Akai, *Applied Numerical Methods for Engineers*, John Wiley and Sons, Inc., New York, NY, 1994

[54] Eugene Isaacson and H. B. Keller, *Analysis of Numerical Methods*, John Wiley and Sons, New York, NY, 1966

[55] A. Morgan, *Solving Polynomial Systems Using Continuation for Engineering and Scientific Computations*, Prentice-Hall, Englewood Cliffs, NJ, 1987

[56] C. B. Garcia, W. I. Zangwill, *Pathway to Solutions, Fixed Points and Equilibria*. Prentice Hall, Eaglewood Cliffs, NJ, 1987

[57] E. L. Allgower and K. Georg, *Numerical Continuation Methods: an introduction*. Springer-Verlag, New York, NY, 1990

[58] C. B. Garcia and T. Y. Li, "On The Number of Solutions to Polynomial Systems of Equations", *SIAM Journal of Numerical Analysis*, vol. 17, no. 41, pp. 540-546. 1980

[59] W. I. Zangwill and C. B. Garcia, *Pathways to Solutions, Fixed Points, and Equilibria*, Prentice-Hall, Englewood cliffs, NJ, 1987

[60] A. Morgan, "A Homotopy for Solving General Polynomial Systems that Respects m-Homogeneous Structure", *Applied Mathematics and Computation*, vol. 24, pp. 101-113, 1987

[61] V. L. Stonick, *Global Methods of Pole/Zero Modeling for Digital Signal Processing Using Homotopy Continuation Methods*, Ph.D dissertation, North Carolina State University, Raleigh, NC, 1989

[62] V. L. Stonick, "Global Optimal Rational Approximation Using Homotopy Continuation Method", *IEEE Transactions on Signal Processing*, vol. 40, no. 9, 1992

[63] Anthony D. Whalen, *Detection of Signals in Noise*, Academic Press, Inc., San Diego, CA, 1971

[64] W. C. Rheinboldt, *An adaptive continuation process for solving systems of nonlinear equations*. Polish Academy of Science. *Banach Ctr. Publ.*, 3, 1977

[65] Danial F. Marshall and W. Kenneth Jenkins, "Fast Quasi-New Adaptive Filtering Algorithms", *IEEE Transactions on Signal Processings*, vol. 40, no. 7, pp. 1652-1662, 1992

[66] R. D. Gitlin and F. R. Magee, Jr., "Self-orthogonalizing adaptive equalization algorithms", *IEEE transactions on Communications*, vol. COM-25, no. 7, pp. 666-672, 1977

[67] R. Bruce Thompson and Donald O. Thompson, "Ultrasonics in Nondestructive Evaluation", *Proceedings of the IEEE*, vol. 73, no. 12, 1985

[68] S. Kraus and K. Goebbels, "Improvement of signal-to-noise ratio for the ultrasonic testing of coarse grained materials by signal averaging techniques", *Proceedings of First International Symposium on Ultrasonic Material Characteristics*, Gaitherburg, June 7, 1978.

[69] R. Murthy, N. M. Bilgutay and J. Saniie, "Aplication of bandpass filtering in ultrasonic nondestructive testing", *Review of Progress in Quantitative Nondestructive Evaluation of Materials*, vol. 8, pp. 759-767, 1989

[70] V. L. Newhouse, N. M. Bilgutay, J. Saniie, and E. S. Furgason, "Flaw-to-grain echo enhancement by split-spectrum processing", *Ultrasonics*, vol. 20, pp. 59-68, 1982

[71] Y. Zhu and J. P. Weight, "Ultrasonic Nondestructive Evaluation of Highly Scattering Materials Using Adaptive Filtering and Detection", *IEEE Transactions on Ultrasonics, Ferroelectrics, and Frequency Control*, vol.41, no.1, pp. 26-33, 1994

[72] Chien-Ping Chiou, R. Bruce Thompson and Lester W. Schmerr, "Ultrasonic Signal-to-Noise Ratio Enhancement Using Adaptive Filtering Technique", *Review of Progress in Quantitative Nondestructive Evaluation of Materials*, vol. 14, 1995

ACKNOWLEDGMENTS

In an old tale, a wise old hermit told a king that the most important people in the world were THE PEOPLE AROUND YOU NOW. I spent the happiest time in my life in Ames on the favor of the people who showed their unsparing understanding of this tale to me, neglecting stupidity and prejudice of mine.

I would like to express my heartfelt thank to Dr. Lalita Udpa, my major professor, and Dr. Satish Udpa, for their essential advice and help through the study of this dissertation. They also offered me the motive and indispensable clues for this study. I also would like to thank committee members, Dr. Fritz Keinert in the Dept. of Mathematics, Dr. William Lord in the Dept. of Electrical Engineering and Dr. William Meeker in the Dept. of Statistics for their kindness and important suggestions during the preliminary examination and through the review of this dissertation.

I also would like to thank to all my friends in the department and Ames community and colleagues in research projects for their consistent encouragement through my life in Ames.

I also thank to my lovely families, father, mother, brother, sisters, sister-in-law and lovely nephew in my home country, and families of my wife, for their ceaseless support and concerns to me, and to my lovely wife Hyunjung and my daughter Kyuwon for everything, and most of all, to the Gods, and Their love and blessings to us.